1970

The relationship between reflectance and surface roughness of printed ink films

Frederick E. Wtherall Jr.
Lehigh University

THE RELATIONSHIP BETWEEN REFLECTANCE AND SURFACE ROUGHNESS OF PRINTED INK FILMS

by
Frederick E. Witherell, Jr.

A Research Report
Presented to the Graduate Faculty
of Lehigh University
in Candidacy for the Degree of
Master of Science

Lehigh University
1970

This research report is accepted and approved in partial fulfillment of the requirements for the degree of Master of Science in Chemical Engineering.

27 MAY 1970

Date

Harry W. Pochlein

Professor in Charge

C. W. Clump

Head of the Department

ACKNOWLEDGEMENT

The author wishes to thank Miss Jaqueline M. Petsko, Assistant Director of the National Printing Ink Research Institute, and Dr. Gary W. Poehlein for their help and guidance throughout the course of this work. Acknowledgement goes also to Dr. William D. Schaeffer, former Director of the National Printing Ink Research Institute, and presently Director of the Graphic Arts Technical Foundation, and Dr. Eugene M. Allen, for their helpful suggestions and discussions.

The financial support of the Boxboard Research and Development Association and the National Printing Ink Research Institute is gratefully acknowledged.

TABLE OF CONTENTS

LIST OF FIGURES

LIST OF TABLES

ABSTRACT

The reflectance properties of printed surfaces, as they are related to surface roughness and configuration, were studied. Specular gloss measurements made on a series of coated and uncoated paperboards, and on prints of varying film thickness on these boards, were related to surface roughness as represented by the number of maxima and minima in Brush roughness profiles. At 20° and 85° incidence a single correlation curve was obtained for all samples, while at intermediate angles separate curves were obtained for the boards, and for each series of prints differing by board type and manufacturer.

Goniophotometer curves were obtained for all samples at 75° and 85° incidence at a wavelength of 578 mμ. For all samples the maximum reflectance occurred at an angle greater than the specular angle, and the reflectance values were lower than the corresponding specular gloss values.

A simplified theoretical model of reflectance from rough surfaces, which considers the surface to be composed of small reflecting facets, was compared with the experimental goniophotometer curves. The agreement was fairly good for most of the samples. Two model parameters, the standard deviation of the facet slope distribution, and the facet area, were determined for each sample by fitting the theoretical curves to the experimental data. In general, the values of these parameters determined for each sample at 75° and 85° incidence did not agree within experimental error, due to the simplified form of the model. Recommendations are presented for a more rigorous theoretical approach to the problem.

1. INTRODUCTION

Gloss and gloss uniformity are assuming increasing importance in the printing and packaging industry because of the value of attractiveness and general appearance of printed objects. Little is known of the relationships between gloss and the multitude of factors which can affect it. Among these factors are pigment particle size, pigment loading, ink film thickness, vehicle viscosity, and stock pore structure. Some exploratory work has been done at the National Printing Ink Research Institute (1-3). This work demonstrates that the inter-relationships between the important variables are complex, but that they all affect the smoothness of the printed film, which is the basic requirement of high gloss and uniformity.

The definition of gloss has caused some confusion in the past, since it can be interpreted in several different ways. Hunter (4) has defined six distinct types of gloss: specular gloss, sheen, contrast gloss, absence of bloom gloss, distinctness of image gloss, and absence of surface texture gloss. Of these, the one which is most commonly applied to ink films is specular gloss, which may be thought of as the degree of approach of the test surface to a mirror surface. Specular gloss is a measure of the intensity of reflection at a reflection angle equal to the incident angle.

Figure 1 illustrates the type of reflection obtained for a perfectly reflecting mirror surface. If light is directed upon the surface at an angle of incidence ψ measured from the normal to the surface, it will be reflected at an angle θ, where θ is equal to ψ.

Figure 2 depicts light incident upon a moderately rough surface. The surface is considered to be composed of small facets oriented at various angles to the mean surface. Each facet is, in turn, considered to be a small

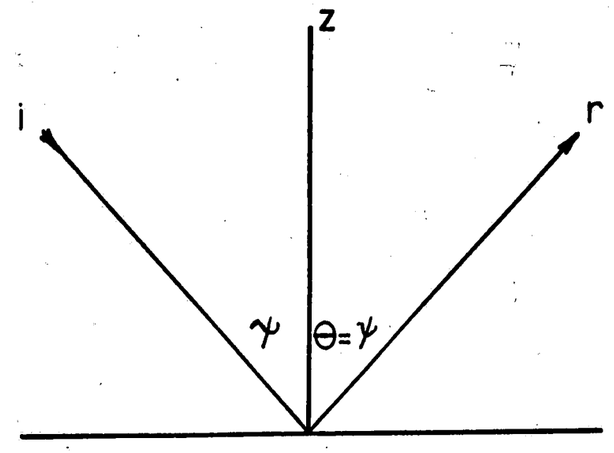

Figure 1: Reflection from a Mirror Surface

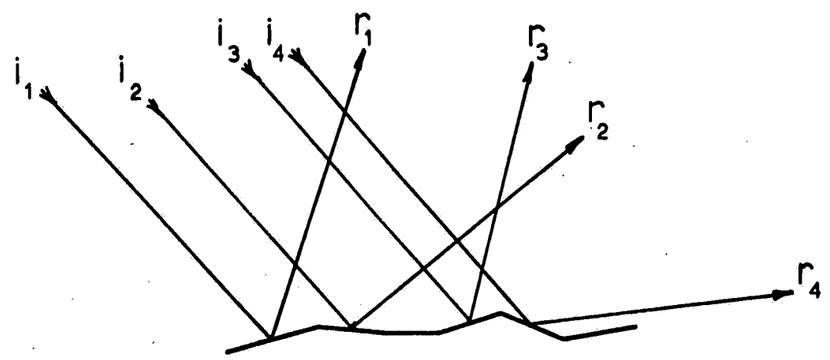

Figure 2: Reflection from a Moderately Rough Surface

mirror similar to that depicted in Figure 1. Therefore, each facet reflects light at a reflection angle equal to the angle of incidence for that particular facet. The resultant reflection from the composite surface is, then, the sum of the reflections from the individual facets. As illustrated in the figure, reflection occurs over a range of reflection angle, θ.

If all facet orientations are equally likely, light incident upon the surface at any angle ψ with respect to the normal to the mean surface plane will be reflected with equal intensity at all angles, θ. Such a surface is called a perfectly diffusing surface, and the intensity of the reflection is given by Lambert's law:

$$R_r = aR_i \cos \psi \qquad (1)$$

where R_r = intensity of the reflected light

R_i = intensity of the incident light

a = constant

All real reflecting surfaces lie between the two extremes of a perfect reflector and a perfect diffusor. That is, the value of the reflectance will vary with the angle of reflection (which will hereafter be referred to as the angle of viewing). Theoretically, by studying the dependence of reflectance on the angle of viewing, for a given angle of incidence, it should be possible to determine the distribution of facet orientations in the surface. The purpose of this research was to deduce the relationship between reflectance, or gloss, and the surface configuration of various paperboards and printed ink films.

The preceding theory does not include several factors which complicate the analysis:

a. multiple reflections between facets

b. masking and shadowing of some facets by their neighbors

c. the fact that print surfaces reflect only a fraction of the light incident upon them, the remainder being transmitted to the complex system of pigment, vehicle, and substrate which lies below the surface

These factors will be discussed in detail in Chapter II.

II. THEORETICAL DISCUSSION

A. Historical Background

The earliest attempt to explain reflection from rough surface was by Bouguer (5), who postulated a surface composed of small mirrors oriented at all possible inclinations to the mean surface. Bouguer examined several surfaces with a simple goniophotometer, and found that they obeyed Lambert's law only very approximately.

This point was taken up by Grabowski (6), who attempted to prove that Lambert's law could not be verified by the Bouguer hypothesis. He assumed that reflection is proportional to the cosine of the viewing angle, and found that in order to explain Lambert's law by the Bouguer hypothesis, Fresnel's law of reflection (7) must be given by

$$F(\gamma) = A \sec^{2n} \gamma \qquad (2)$$

where A, n = constants

γ = angle of incidence

Grabowski stated that this expression is impossible. F is an increasing function, and thus, n must be positive. But if so, $F(\gamma) = \infty$ at $\gamma = \frac{\pi}{2}$, which is incorrect. Therefore, Grabowski concluded, the Bouguer hypothesis cannot be employed to explain Lambert's law.

Berry (8) expressed the opinion that Grabowski's arguments did not necessarily invalidate Bouguer's theory, since physical laws are only approximations of actual behavior, and often fail in limiting cases. He defined several types of "ideally rough" surfaces statistically, calculated the laws which govern diffuse reflection from these surfaces, and compared these with

experimental results. The disagreements were considerable in some cases, but Berry stated that the discrepancies may arise from shadowing of some facets by neighboring facets. He concluded that the agreement is probably as good as could be expected, and that Bouguer's hypothesis need not be discarded.

Chinmayanandam (9) described a rough surface as one having reflecting elements who heights are distributed according to the Gaussian probability law. He derived an expression for reflection for this model which yields fairly good agreement with experiment for incident and viewing angles up to 54°:

$$R = e^{-(8\pi^2 \cos^2 \theta)/\alpha\lambda^2} \qquad (3)$$

where θ = viewing angle

λ = wavelength of radiation

α = experimental constant

For larger angles, Chinmayanandam concluded that shadowing effects became important, and he employed a complex empirical formula which gave good agreement with experiment.

Pokrowski (10-13) undertook an extensive study of the problem, making the following assumptions:

a. a portion of the light is directly reflected from the surface

b. the remainder of the light is diffused from the interior of the material

c. Fresnel's law can be used to determine the amount of light reflected from the surface for a given incidence angle-viewing angle combination

d. all facet orientations are equally likely

e. the light diffused from within the body obeys Lambert's law

Thus, Pokrowski's result was:

$$R = a \cdot F + b \cos \gamma \qquad (4)$$

where F = Fresnel's law

a,b = experimental constants

He presented data for 80° incidence which showed good agreement with Equation 4, and discussed the importance of shadowing, multiple reflections between facets, and absorption of light in the interior of the material.

Schulz (14) held that several of Pokrowski's assumptions, particularly that of a uniform facet orientation distribution, were not realistic. He assumed that the reflectance consisted of surface reflection, regular reflection from particles within the material, and diffuse reflection from below the surface. Schulz also modified Pokrowski's equation to account for shadowing by neighboring facets.

Barkas (15) extended the work of Pokrowski and Schulz, assuming a surface composed of specularly and diffusely reflecting facets, the latter to account for scattering and multiple reflections. He arrived at the following expression for reflectance:

$$R = \frac{r\,A}{2 \cos \gamma} \left\{ \cos (\gamma - \theta) + \cos (\gamma + \theta) \right\} + F\,B \cos \left[\tfrac{1}{2} (\gamma - \theta) \right] \qquad (5)$$

where A = area, per cm^2 of mean surface, of rough facets illuminated and visible for particular values of γ and θ

B = the similarly defined area of mirror facets

r = the proportion of incident light scattered normally to a rough facet

F = Fresnel's law

The agreement was fairly good for the materials tested.

Bennet and Porteus (16-18) developed a theory for the relationship between surface roughness and specular reflection at normal incidence. The theory is applicable when the root-mean-square surface roughness is small compared to the wavelength of light (34). The equation derived was:

$$R = R_i \exp\left[-(4\pi\sigma)^2/\lambda^2\right] + R_i \frac{2^5\pi^4}{m^2} (\sigma/\lambda)^4 (\Delta\theta)^2 \qquad (6)$$

where R_i = intensity of incident light

σ = root mean square surface roughness

λ = wavelength of incident light

m = root mean square slope of the surface profile

$\Delta\theta$ = instrumental acceptance angle

A considerable amount of work has been done in the Soviet Union (19-24) concerning specular reflection of polarized light from rough dielectric surfaces. All of this work was concerned, to a great extent, with diffraction effects. Gordinskii (19) considered the problem from the point of view of statistical interference of coherent (i.e. identical) sources of reflection in the surface. He derived the following expression for specular reflection:

$$\rho_{rel} = e^{-qk^2} \qquad (7)$$

where ρ_{rel} = ratio of specularly reflected light from the rough surface to specularly reflected light from a polished surface

q = index of roughness

$= 8\pi^2\sigma^2$

σ = standard deviation of the statistical distribution of roughness heights (assumed to be Gaussian)

k = index of interference

$= \frac{\cos\gamma}{\lambda}$

Toporets (20, 23) observed specular peaks in goniophotometer curves with polarized light for roughened ($h \approx 12\mu$), but not polished, ground glass surfaces. He interpreted this as indicating ordinary Fresnel specular reflection distorted by diffraction. In addition, the specular maxima of the curves decreased, and their half-widths increased, with increasing angle of incidence, a result which is exactly the opposite of that which is generally observed. Using a very precise goniophotometer (angular aperture of the light beam = 9 min.) Toporets determined the angular distribution of surface facets. He was also able to determine the effective facet size for the roughly polished surfaces.

Voishvillo (22) studied reflection from roughened gray and white glasses at large angles of incidence ($\psi \geq 60^{\circ}$). He observed goniophotometer curves possessing two maxima, one at the specular angle, and one at a higher angle. He assigned the sharp maximum at the specular angle to specular reflection, and the second maximum, which is more or less pronounced depending on surface roughness, to diffuse reflection. He derived the following expression for the diffuse component of reflection:

$$R_d = \frac{r\, E_o\, S_o\, f(\varsigma)}{4} \qquad (8)$$

where r = reflection coefficient calculated by Fresnel's law

E_o = illumination of the projection of a surface facet in a direction perpendicular to the incident beam.

S_o = area of the rough surface which is illuminated

ς = angle between the normals to the mean surface and the facet

$f(\varsigma)$ = distribution of surface facet orientations

Polyanskii and coworkers (21, 24) studied the depolarization of light reflected from rough surfaces, and succeeded in separating the partial reflectances attributable to diffraction and Fresnel reflection. If the specular peak is produced by regular reflection from facets, it will not be depolarized. Such is not the case for diffuse reflection. These workers found that both Fresnel and diffraction mechanisms enter into the formation of the specular peaks.

Nelson and Goulard (25) studied reflection from a periodic dielectric surface with a sine wave as its cross-section. They obtained goniophotometer curves which, in general, had two peaks, one on either side of the specular angle. They concluded that the peaks were caused by reflection from the inflection points of the periodic surface. The magnitude of the off-specular peaks depended almost entirely on, and varied directly with, the index of refraction of the reflecting material. The angular position of the peaks depended upon the radius of curvature of the surface near its peaks, the position approaching the specular angle as the radius of curvature increased.

A great deal of significant work has been done by Torrance and coworkers (26-33, 41) concerning hemispherical reflection from rough metallic and dielectric surfaces. Assuming a Gaussian distribution with rotational symmetry for the facet orientation, the most probable orientation being parallel to the mean surface, they derived an expression for relative reflectance which in the plane of incidence, simplifies to:

$$\frac{\rho(\psi, \theta)}{\rho(\psi, \psi)} = \frac{g\, F(\psi', \hat{n}) \left[G(\psi, \theta)/\cos\theta \right] \exp(-c^2\alpha^2) + \cos\psi}{g \left[F(\psi', \hat{n})/\cos\psi \right] + \cos\psi} \qquad (9)$$

where $\rho(\psi,\theta)$ = reflectance at incident angle ψ and viewing angle θ

$\rho(\psi,\psi)$ = reflectance at the specular angle

$F(\gamma', \hat{n})$ = Fresnel's law

γ' = angle of incidence with respect to the facet

$= \frac{\gamma + \theta}{2}$

$\hat{n}$ = complex index of refraction, composed of the real index of refraction, and the coefficient of absorption

$G(\gamma, \theta)$ = geometrical attenuation factor, which accounts for masking and shadowing effects

α = facet orientation angle, equal to the angle between the normals to the mean surface and the facet

$= \frac{\theta - \gamma}{2}$

c, g = experimental constants

Agreement with experiment was good for several types of metallic and dielectric surfaces.

Harrison (35) has presented an excellent survey of the early work done in the field of gloss measurement.

It is apparent that, although each of the models presented here has proved satisfactory for certain types of surfaces, no theory has yet been developed which adequately describes all surfaces. In addition, no model has been developed to describe the reflectance properties of rough printed surfaces. It is to this end that the present research was directed.

B. Development of Surface Configuration-Reflectance Relationship

1. The Normal Distribution

The normal, or Gaussian, probability distribution is given by Equation 10 (30):

$$P(\alpha) = \frac{1}{\sigma\sqrt{2\pi}} \exp\left[-\frac{1}{2}\left(\frac{\alpha - \mu}{\sigma}\right)^2\right] \qquad (10)$$

where α = the independent variable

μ, σ = mean and standard deviation, respectively

The mean μ of a probability distribution is defined as the expectation of the probability distribution, or in simple terms, as the average value of α. For many systems the mean will assume a value of zero. That is, a plot of $P(\alpha)$ versus α will be symmetric about the point $\alpha = 0$. Thus,

$$P(\alpha) = \frac{1}{\sigma\sqrt{2\pi}} \exp\left(-\frac{\alpha^2}{2\sigma^2}\right) \qquad (11)$$

The significance of the standard deviation σ is illustrated in Figure 3, which is a plot of the normalized Gaussian distribution, $P(t)$, where $t = \frac{\alpha}{\sigma}$. The area under the curve between any two values of t gives the probability that t lies between those limits. Thus the area between $t = \pm 1$ is the probability of α being within one standard deviation of the mean, the area between $t = \pm 2$ is the probability of α being within two standard deviations of the mean, etc. The standard deviation, then, is a measure of the width of the probability distribution. The area under the curve of Figure 3 between $t = \pm 1$ is approximately 0.683. Since the total area beneath the curve is 1.0, α assumes a value within one standard deviation of the mean 68.3% of the time. Similarly, α will assume a value within two standard deviations of the mean 95.4% of the time, and will virtually always be within three standard deviations of μ (99.7%).

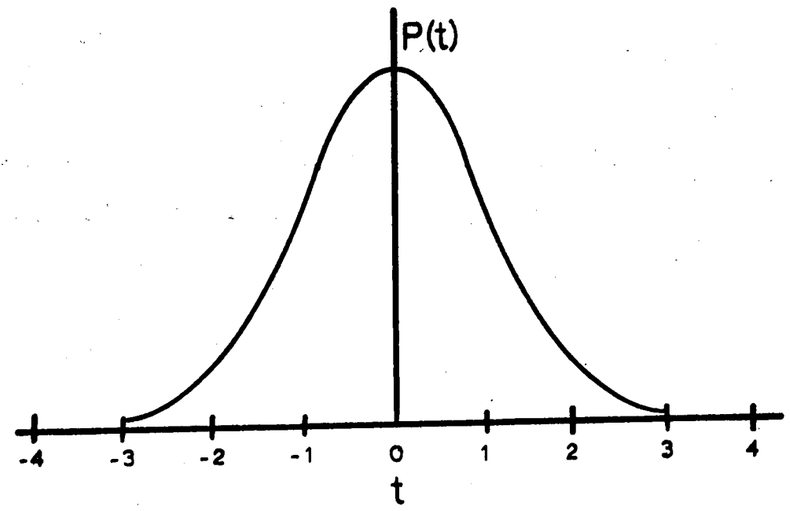

Figure 3: Normalized Gaussian Distribution

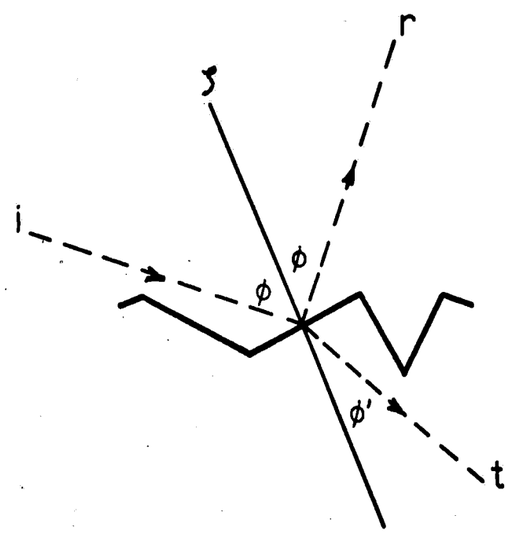

Figure 4: Incident, Reflected, and Transmitted Rays at a Facet

2. Surface Theory

Consider a rough surface to be composed of numerous small facets, as shown in Figure 4, which reflect a portion of the light incident upon them, transmitting the remainder into the interior of the substrate. The reflected light is composed, therefore, of light specularly reflected from the facets, light multiplyreflected between facets, and light scattered from pigment particles and board fibers below the surface. The latter two phenomena are grouped together to form the diffuse portion of the reflectance.

Figure 5 depicts a small area of surface δS which contains many facets. The normal to δS will be called z. Light is incident upon δS at an angle ψ measured from z, and reflectance is measured at a viewing angle θ. The incident beam i, the reflected beam r, and z, are all in the same plane, known as the plane of incidence. The time averaged rate of flow of radiant energy from a light source of radiance N_i, incident at an angle ψ, which falls within an elementary solid angle $\delta\Omega_i$ and is incident on the surface element δS is

$$\delta\Phi_i = N_i \delta\Omega_i \delta S \cos\psi \tag{12}$$

Similarly, for the reflected radiant energy flow rate,

$$\delta\Phi_r = \delta N_r \delta\Omega_r \delta S \cos\theta \tag{13}$$

δN_r is employed to emphasize that while the radiance of the source is assumed constant over its entire area, the radiance of the reflecting surface is not. Thus δN_r will vary with position on the surface, and with the incident and viewing angles, and only a small surface area can be considered at any one geometry.

Reflectance is defined as the ratio of the reflected to the incident radiant energy flow rates (37):

$$\delta\rho = \frac{\delta\Phi_r}{\delta\Phi_i} \tag{14}$$

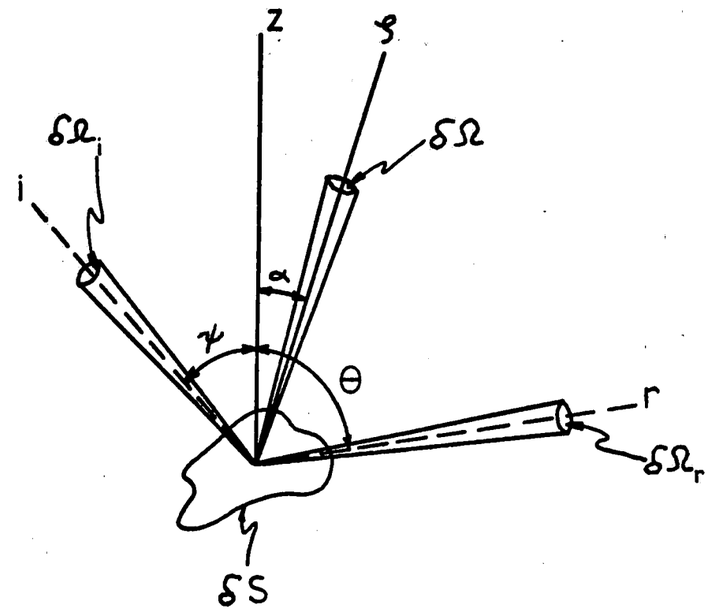

Figure 5: Geometry at the Surface

or, when considered as percent reflectance (gloss):

$$\delta\rho = 100 \frac{\delta \Phi_r}{\delta \Phi_i} \tag{15}$$

Substituting Equations 12 and 13 into Equation 15 yields the following expression for percent reflectance:

$$\delta\rho = 100 \frac{\delta N_r \, \delta\Omega_r \cos\theta}{N_i \, \delta\Omega_i \cos\gamma} \tag{16}$$

Those facets in δS which accept light within $\delta\Omega_i$ and reflect it specularly within $\delta\Omega_r$ must possess normals γ within $\delta\Omega$. The angle between z and the normals to these facets is called the facet orientation angle, and is given the symbol α, where

$$\alpha = \frac{\theta - \gamma}{2} \tag{17}$$

Let $P(\alpha)\delta\Omega$ be the number of facets per unit surface area with normals within $\delta\Omega$, where $P(\alpha)$ is assumed to be the normal distribution with mean zero:

$$P(\alpha) = \frac{1}{\sigma\sqrt{2\pi}} \exp\left(-\frac{\alpha^2}{2\sigma^2}\right) \tag{11}$$

The number of facets within δS with normals within $\delta\Omega$ is

$$a P(\alpha) \, \delta\Omega \, \dot{\delta} S$$

Assuming all facets to be of equal area a, the total reflecting area of the facets is

$$a P(\alpha) \, \delta\Omega \, \delta S$$

and its projection in the direction of the source is

$$P(\alpha) \delta\Omega \, \delta S \cos\phi$$

where ϕ = the angle of incidence to the facet

$$= \frac{\gamma + \theta}{2}$$

Therefore, the rate of radiant energy flow incident upon these facets is

$$\delta \Phi_i = a N_i P(\alpha) \delta \Omega_i \delta \Omega \delta S \cos \phi \tag{18}$$

As previously indicated, the surface facets will reflect only a portion of the incident radiant energy, the remainder being transmitted to the pigment and board fibers below. The reflected fraction is represented by Fresnel's law, which, for a particular facet orientation, may be given as (7).

$$F = \frac{1}{2}\left[\frac{\sin^2(\phi - \phi')}{\sin^2(\phi + \phi')} + \frac{\tan^2(\phi - \phi')}{\tan^2(\phi + \phi')}\right] \tag{19}$$

where ϕ' = angle between the transmitted ray and the facet normal (angle of transmission) as shown in Figure 4

$= \arcsin\left(\frac{\sin \phi}{n}\right)$

n = index of refraction of the reflecting medium

The angle of incidence, ϕ, is as defined above. Therefore, the rate of flow of radiant energy specularly reflected is

$$\delta \Phi_{r,s} = F \delta \Phi_i(\psi) \tag{20}$$

Two other phenomena which occur at the surface have not yet been mentioned. These are masking, which is the obstruction of reflected radiation from a facet by an adjacent facet, and shadowing, which is the blocking of incident radiation to a facet by an adjacent facet. These phenomena are illustrated in Figure 6. They are functions of the incident and viewing angles, and are represented by the geometrical attenuation factor G. The analytical expression for G has been derived by Torrance and Sparrow (33) with the following simplifying assumptions:

a. the root-mean-square surface roughness is comparable to, or greater than, the wavelength of the incident light

a)

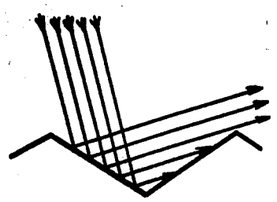

b)

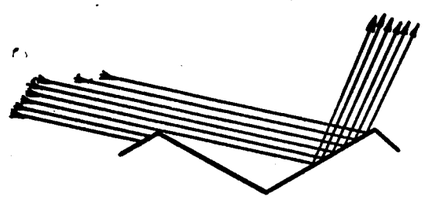

c)

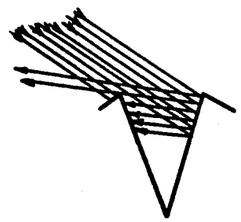

Figure 6: a) masking
b) shadowing
c) masking and shadowing

b. each facet forms one side of a symmetric V-groove cavity

c. the longitudinal axis of each cavity is parallel to the plane of the mean surface

d. the upper edges of all cavities lie in the same plane

G is the fraction of the illuminated facet that actually contributes to the reflected intensity, and is given by Equation 21:

$$G = 1 - \frac{1 - (1 - A^2)^{\frac{1}{2}}}{A} \tag{21}$$

where A depends upon the geometry as follows:

a. $\pi/4 \leq \psi \leq \pi/2$, $0 \leq \theta \leq \psi - \pi$

$$A = \frac{\sin^2 \psi - \cos^2 [(\psi - \theta)/2]}{\cos^2 [(\psi - \theta)/2] - \cos(\psi - \theta) \sin^2 \psi} \tag{22a}$$

b. $0 \leq \psi \leq \pi/4$, $0 \leq \theta \leq (\psi + \pi)/3$; and $\pi/4 \leq \psi \leq \pi/2$, $3\psi - \pi \leq \theta \leq (\psi + \pi)/3$

$$A = 0 \tag{22b}$$

c. $0 \leq \psi \leq \pi/2$, $(\psi + \pi)/3 \leq \theta \leq \pi/2$

$$A = \frac{\sin^2 \theta - \cos^2 [(\theta - \psi)/2]}{\cos^2 [(\theta - \psi)/2] - \cos(\theta - \psi) \sin^2 \theta} \tag{22c}$$

Inclusion of Equation 18 and the geometrical attenuation factor in Equation 20 yields

$$\delta \Phi_{r,s} = F G a N_i P(\alpha) \delta \Omega_i \delta \Omega \delta S \cos \phi \tag{23}$$

But by Equation 13

$$\delta \Phi_{r,s} = \delta N_{r,s} \delta \Omega_r \delta S \cos \theta \tag{24}$$

and, following Rense (38)

$$\delta \Omega = \frac{\delta \Omega_r}{4 \cos \phi} \tag{25}$$

Therefore

$$\delta N_{r,s} = \frac{a}{4\sigma\sqrt{2\pi}\cos\theta} F G N_i \exp\left(-\frac{\alpha^2}{2\sigma^2}\right)\delta\Omega_i \qquad (26)$$

The diffuse radiance term may be assumed to follow Lambert's law:

$$\delta N_{r,d} = k N_i \cos\psi \, \delta\Omega_i \qquad (27)$$

Substitution of Equations 26 and 27 into Equation 16 yields the expression for percent reflectance for the small solid angle of reflectance $\delta\Omega_r$:

$$\delta\rho = 100\left[\frac{a}{4\sigma\sqrt{2\pi}\cos\psi} F G \exp\left(-\frac{\alpha^2}{2\sigma^2}\right)\delta\Omega_r + k\cos\theta\,\delta\Omega_r\right] \qquad (28)$$

To obtain the actual percent reflectance, $\delta\Omega_r$ must be replaced by the solid angle Ω_r actually subtended by the receptor of the instrument employed for the measurements. This is done by summing Equation 28 over all values $\delta\Omega_r$ for a given geometry, or by reducing $\delta\rho$ and $\delta\Omega_r$ to the differential quantities $d\rho$ and $d\Omega_r$ and integrating. In either case, if the receptor is small enough, all factors in Equation 28 can be considered constant for given values of ψ and θ, and the result is

$$\rho = 100\left[\frac{a}{4\sigma\sqrt{2\pi}\cos\psi} F G \exp\left(-\frac{\alpha^2}{2\sigma^2}\right)\Omega_r + k\cos\theta\,\Omega_r\right] \qquad (29)$$

III. EXPERIMENTAL

A. Materials

1. Paperboards

Samples of thirteen different paperboards, of which seven were coated boards, were obtained from two manufacturers. The boards varied widely in smoothness, texture, and gloss; the coated boards generally presenting the smoothest and glossiest finish. Property variations were obtained during manufacture employing different calendar solutions on the uncoated grades, and by varying the binder level on the coated grades.

2. Ink

The ink was a single sample of a gloss-testing orange (Interchem Printing Inks, Division of Interchemical Corporation, Elizabeth, New Jersey). The ink had good gloss differentiation properties. A spectral reflectance curve for the ink on a print exhibiting full coverage appears in Figure 7.

B. Equipment

1. Surface Roughness Analyzer

Surface roughness measurements were made with the Brush Surface Analyzer, model MS-5000 (Brush Instruments Division, Clevite Corporation, Cleveland, Ohio). The instrument employs a diamond stylus probe, model MS-1100, with a stylus radius of 0.0005 inch. The stylus is operated by an electro-hydraulic probe drive, model MS-1400, with adjustable stroke length and speed. The sensitivity is controlled by a surfindicator, model MS-1000, which is connected to a Mark II recorder. The recorder has an adjustable chart speed, and employs electric styli to give separate traces of roughness and either root-mean-square average or arithmetic average roughness on hear sensitive chart paper.

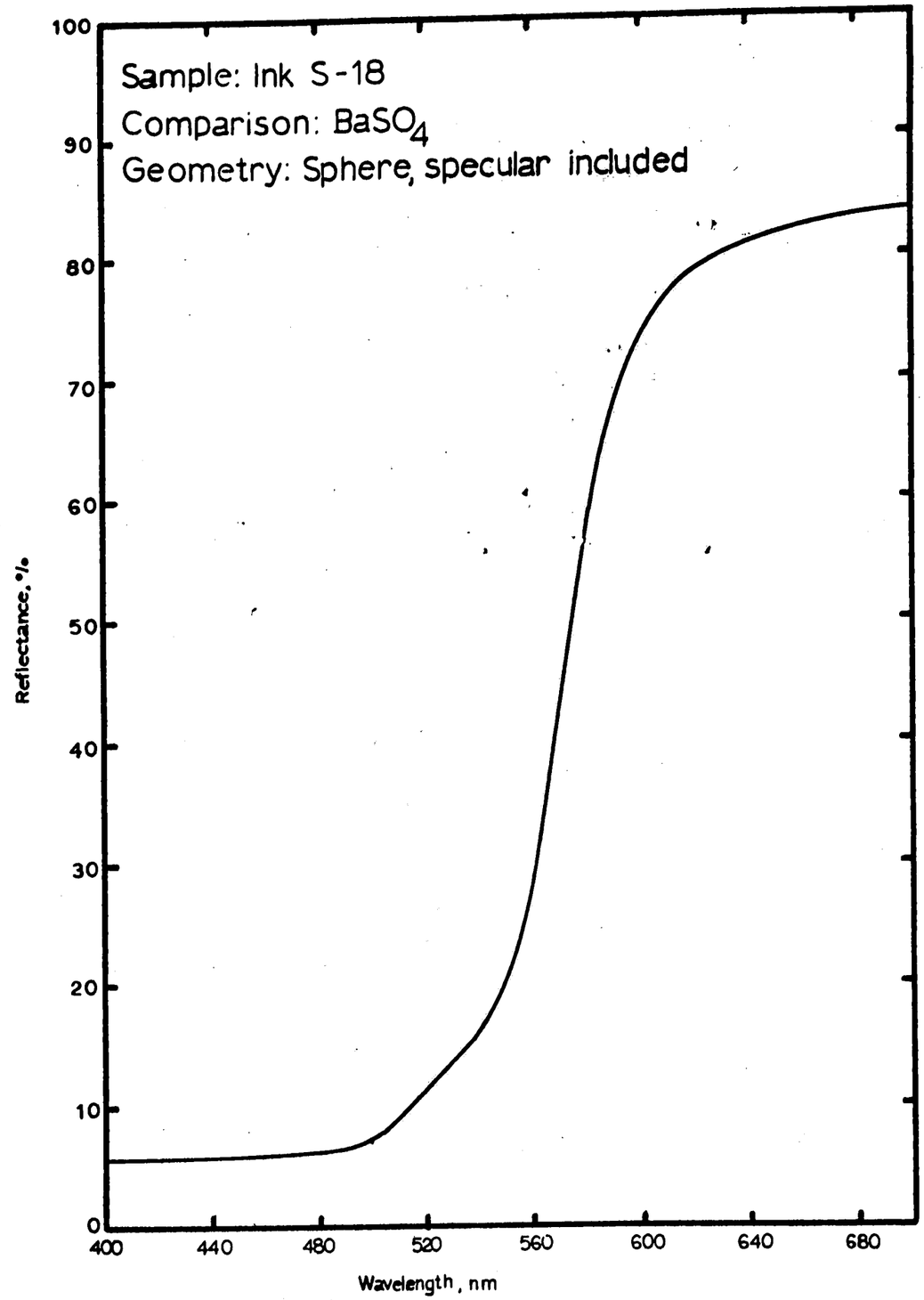

Figure 7: Spectral Reflectance Curve for Gloss-Testing Ink S-18

2. Specular Glossmeter

Specular gloss was measured with Gardner Multi-angle Glossmeter, model GG-9095 (Gardner Laboratories, Inc., Bethesda, Md.). The instrument employs white incandescent light, and can measure specular gloss at 20°, 45°, 60°, 75°, and 85°. A polished black carrara glass tile was used as a standard for calibration. The source apertures for both 75° and 85° are circular, and 0.8 cm. in diameter. The 75° receptor aperture is circular, with a diameter of 2.8 cm., while that for 85° is rectangular, with dimensions of 1.4 cm. x 1.0 cm.

3. Goniophotometer

A Brice-Phoenix Universal Light Scattering Photometer, series 1999-7 (Phoenix Precision Instruments Co., Philadelphia, Pa.) was modified for use as a goniophotometer. The instrument employs a mercury-vapor light source, contains four neutral filters of known transmittances to control incident intensity, and has several filter systems for isolating various shades of monochromatic radiation. Readings are obtained on a galvanometer connected to the photoelectric cell of the receptor.

A source aperture of dimensions 1.5 cm. x 0.4 cm. was employed for reflectance measurements in the machine direction. The aperture width was reduced to 0.2 cm. for measurements across the machine direction, since the samples were narrower in this direction. The receptor dimensions of 1.0 cm. x 0.3 cm. were the same in both cases. A schematic diagram of the apparatus is shown in Figure 8.

Since the instrument was not originally designed for this type of work, a plexiglass sample holder was constructed. This device consisted of

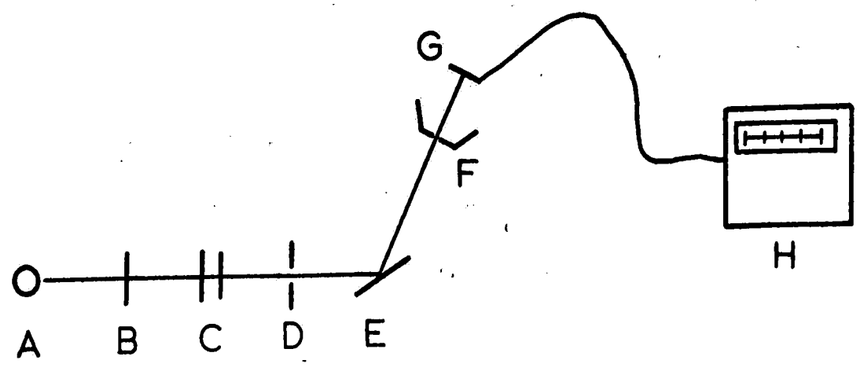

Figure 8: Schematic Diagram of the Modified Brice-Phoenix Light Scattering Photometer: A) Mercury vapor light source, B) color filters, C) neutral filters, D) collimating slit, E) sample, F) receptor slit, G) photoelectric cell, H) galvanometer

two parts: a square, flat base on which protractor markings were carved, and which fit snugly into the sample compartment, and an upright section, which rotated on a pin projected upward from the base, to which the sample was secured. A sketch of the sample holder is shown in Figure 9. A polished black carrara glass tile was used as a standard for calibrating the instrument.

C. Experimental Procedures

1. Surface Roughness Measurements

The probe automatic drive on the Brush Surface Analyzer was adjusted to a stroke length of 0.5 inch, and a stroke speed of 1/80 inch/sec. A chart sensitivity of 20 micro-inches (approximately 0.5 microns) per chart division, and a chart speed of 5 mm/sec. for coated boards and their prints, and 25 mm/sec. for uncoated boards and their prints, were found to give the most satisfactory combination of accuracy and chart readability. A trace was first made near the center of the sample, in the machine direction; then the sample was rotated 90°, and a trace was made in the same area of the sample, across the machine direction. In this manner, roughness and root-mean-square roughness traces were made on all board and print samples, in and across the machine direction. A typical trace is reproduced in Figure 10.

The traces were analyzed by counting the total number of maxima and minima in the trace. This number was designated as the roughness of the sample.

2. Specular Gloss Measurements

A polished black carrara glass standard was placed over the aperture of the glossmeter, the selector knob was set at the angle of interest, and the calibration dial was adjusted until the correct standard gloss value was

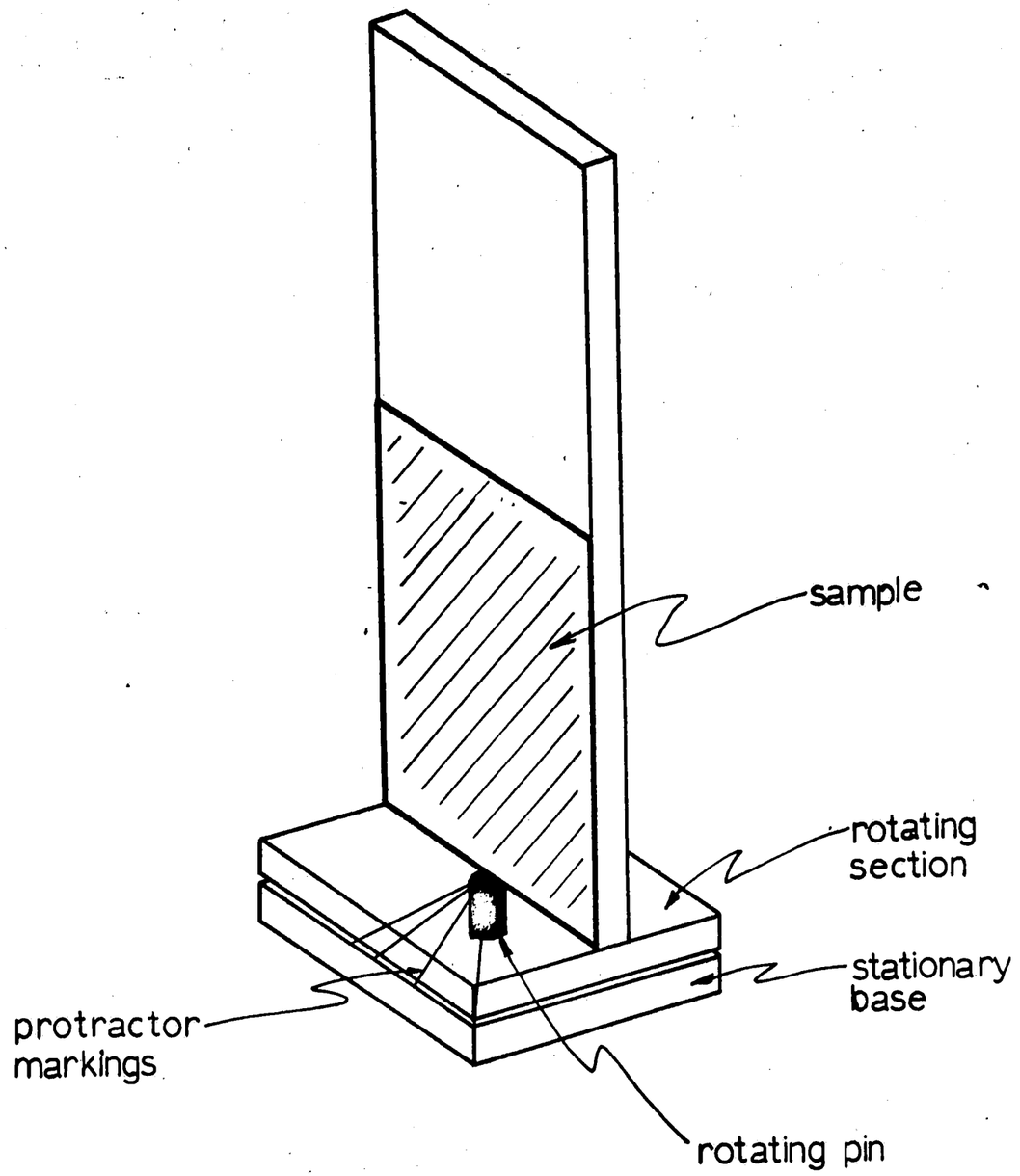

Figure 9: Goniophotometer Sample Holder

A

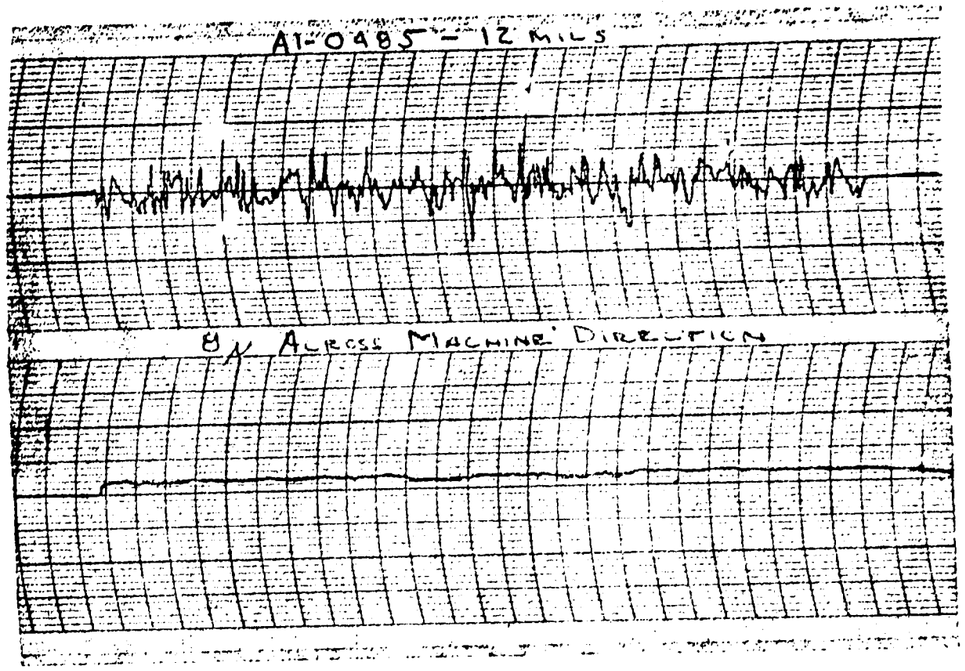

B

Figure 10: Typical Brush Roughness Trace
A) Roughness
B) Root-mean-square Roughness

indicated on the meter (e.g., 99% for 75°, 100% for 85°, etc.). The standard was replaced with a board or print sample aligned in the machine direction, and the gloss value from the meter was recorded. The sample was then rotated 90°, and a gloss value across the machine direction was obtained. This procedure was repeated for all samples at all angles.

3. Goniophotometer Measurements

The 578 m μ filter system was chosen for use with photometer, since it most nearly approximated the pigment color. This system consisted of two component filters, one red-yellow and one blue-green. After this filter system was in place, the apparatus was calibrated. Neutral filter 1-3 were inserted to attenuate the incident beam. A polished black carrara glass standard was placed in the sample holder and the holder was adjusted to the appropriate incident angle (75° or 85°). With the shutter closed to block the incident beam, the galvanometer reading was adjusted to zero. The receptor was then set at the specular angle, the shutter was opened, and the coarse and fine adjustments were utilized to set the galvanometer reading to 10.0. This standardization procedure was repeated at half-hour intervals during use.

With the shutter closed, the standard was replaced by a board or print sample. The receptor was set at a viewing angle of 45°, the shutter was opened, and the neutral filters were adjusted to give the largest on-scale reading attainable. The viewing angle was increased at 5° intervals, the neutral filters being continually adjusted to keep the galvanometer reading on scale, until a viewing angle 5° less than the specular angle was attained. Thereafter, the viewing angle was increased at 1° intervals until 90° was reached. This procedure was repeated with the same sample three additional

times, once as given above, and twice with the sample rotated 180°. Therefore, the reflectance values obtained were the average of four separate readings, a procedure necessitated by the inconsistencies in the board surfaces.

The galvanometer intensity is defined as the galvanometer reading, G, divided by the product of the transmittances τ_i of the neutral filters in place when the reading was taken:

$$I = \frac{G}{\tau_1 \tau_i} \tag{30}$$

The specular reflectance value of the standard, ρ_{st}, is known, and the intensities of the standard, I_{st}, and sample, I_{sa}, are known through Equation 30. Therefore, the sample reflectance at any viewing angle, ρ_{sa}, is given by

$$\rho_{sa} = \frac{\rho_{st}}{I_{st}} I_{sa} \tag{31}$$

D. Determination of Roughness-Reflectance Parameters

Equation 29 contains three parameters which must be determined. a and σ are associated with specular reflectance, and k is associated with the diffuse term. The diffuse term is a constant, indicating that as the specular term decays to low values, the reflectance should decay to a constant, measureable value. As will be discussed more fully in Chapter IV, the experimental curves obtained in this work decay to zero at viewing angles below about 60°. Thus, the diffuse term can be safely ignored in the calculation of theoretical reflectance curves. Setting k equal to zero, Equation 29 becomes

$$\rho = \frac{10\ a}{\sigma \cos \gamma} F G \exp\left(-\frac{\alpha^2}{2\sigma^2}\right) \Omega_r \tag{32}$$

The receptor solid angle Ω_r must be determined before this equation can be used:

$$\tan \frac{\Omega_r}{2} = \tan \frac{\frac{1}{2} \text{ receptor width}}{\text{path length from sample to receptor}}$$

$$= \frac{1.5 \text{ mm}}{35 \text{ mm}} \tag{33}$$

$$= 0.043 \text{ steradians}$$

But for small angles, $\tan \theta \approx \theta$. Therefore,

$$\Omega_r \approx 0.086 \text{ steradians} \tag{34}$$

Thus, Equation 32 becomes

$$\rho = \frac{0.86\, a}{\sigma \cos \gamma} \; F\, G \exp\left(-\frac{\alpha^2}{2\sigma^2}\right) \tag{35}$$

The value of the standard deviation for each sample was determined by calculating reflectance curves, with Equation 35, and choosing the value of σ which caused the calculated reflectance maximum to occur at the same viewing angle, θ_{max}, as the experimental maximum. Such curves were calculated for incidence angles of 75° and 85°. Because the photometer used was not originally designed for use as a goniophotometer, the angle measurements are accurate only to about $\pm$ 1°. Thus a range of σ values was obtained over the viewing angle range $\theta_{max} \pm 1°$.

The range of facet area values "a", for each sample, was then determined. Since the calculated curves only approximately reproduced the shape of the experimental curves, as will be discussed further in Chapter IV, and since the experimental reflectance values were accurate to $\pm$ 10%, the range of values of a determined for each sample was that range which yielded specular reflectance values within 10% of those obtained experimentally. Specular reflectance was chosen, rather than maximum reflectance, since this criterion

seemed to yield beter overall correspondence between the shapes of the experimental and calculated curves.

In calculating reflectance curves for the boards a refractive index of 1.56 was employed (42), while for the prints, the refractive index of the vehicle was taken as 1.44 (43).

IV. RESULTS AND DISCUSSION

A. Brush Roughness - Specular Gloss Relationships

Specular gloss measurements on all boards, and on prints made with 8 and 12 micron ink film thicknesses on the plate, were plotted versus Brush roughness measurements. The resulting plots at 45°, 60°, 75°, and 85° incidence in the machine direction are given in Figures 11 and 12. In general, specular gloss increased with increasing angle of incidence through 75°, and decreased at 85°. As the figures indicate, the decrease in gloss at 85° was more significant for the prints than for the boards. Also, specular gloss generally increased with decreasing roughness. However, at 45°, 60°, and 75° incidence, this decrease followed separate correlation curves for the boards, and for each series of prints differing by board type (coated or uncoated) and manufacturer. At 20° and 85° incidence all boards and prints fell close to a single correlation curve. For glossy boards, print gloss was generally lower than board gloss. The opposite effect was observed for the matte boards.

No satisfactory explanation can be offered for the decrease in gloss at 85° incidence. Fresnel's law, Equation 19, predicts increasing reflection with increasing angle of incidence. Thus it would be expected that 85° gloss should be higher than 75° gloss.

Single correlation curves at 20° and 85° incidence are probably due to very low, and very high, reflection, respectively, at these angles. In the former case, gloss never went beyond 4.5%, and the reflectance was too low to distinguish between differences in surface configuration among the samples. In the latter case Fresnel's law predicts very high reflection, and differences in surface configuration may be masked by this high reflectance.

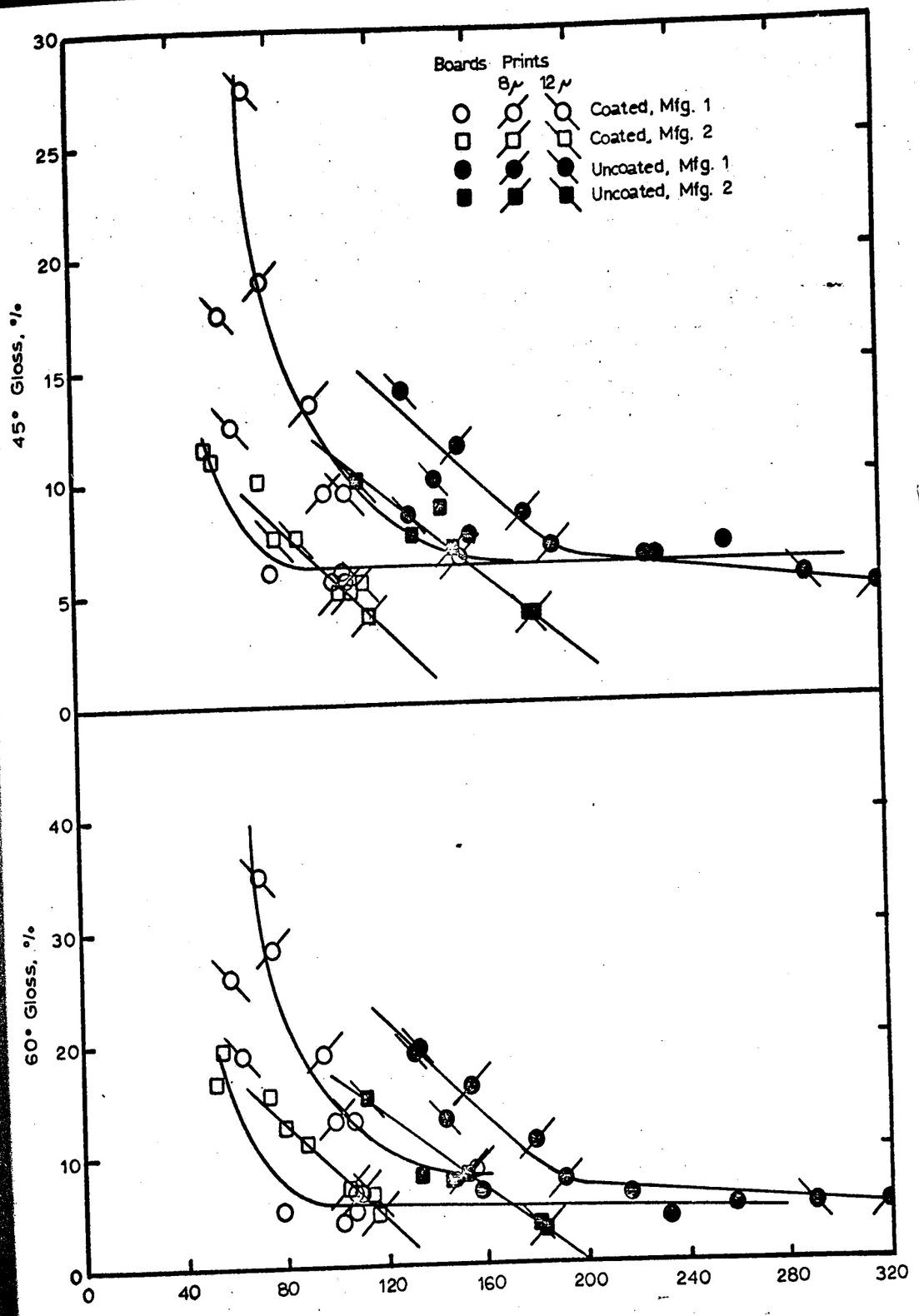

Figure 11: Gloss as a Function of Roughness: Boards and 12 Mil Prints in the Machine Direction 45° and 60° Incidence

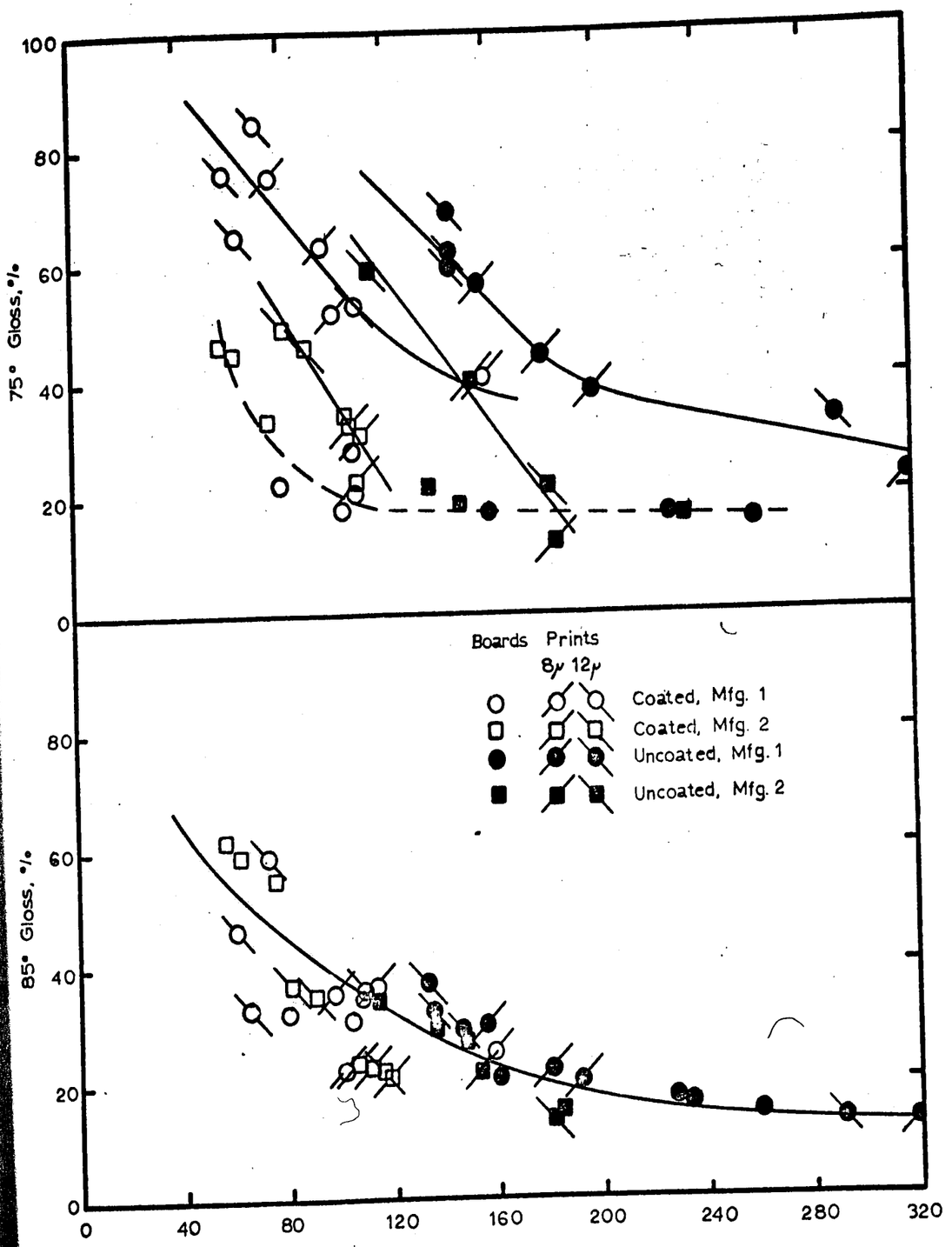

Maxima and minima in 0.5 inch of sample

Figure 12: Gloss as a Function of Roughness: Boards and 12 Mil Prints In the Machine Direction, 75° and 85° Incidence

The ink appeared to hide the gloss of glossy boards, while enhancing that of matte boards.

B. Experimental vs. Calculated Reflectance Curves

Experimental reflectance curves for all boards and printed samples, in and across the machine direction, at 75° and 85° incidence, are included in Appendix A. The curves exhibit maximum reflectance at a viewing angle θ_{max} which is somewhat larger than the specular angle. The calculated curves generally approximate the shape of the experimental curves, with several qualifications. The calculated curves drop off to zero at a viewing angle of 90°, while the experimental curves do not. Also, for values of σ greater than approximately 4.5, the 85° calculated curves reach a sharp maximum at about 88°, then drop off sharply to zero. The experimental 85° curves generally do not exhibit such a sharp maximum, or drop off as rapidly beyond this maximum.

Tables I - IV in Appendix B give the values of standard deviation and facet area for the print samples in the machine direction. Since the standard deviation and facet area are properties of the surface, and are not dependent upon incident angle, it is expected that analysis of each sample should yield the same value of σ and a, within experimental error, at 75° or 85° incidence. Such a result was almost never observed. Indeed, it was often impossible to determine the upper bound of the range of σ for the 85° curves, due to the shapes of the calculated curves. The σ values agreed, within experimental error, in only three cases, while the values of a did not agree for any of the samples tested. The σ and a values were always significantly greater at 75° incidence than at 85°.

Figure 13 is a plot of gloss versus standard deviation for the print samples. In general, gloss decreased with increasing standard deviation. The similarities between Figures 12 and 13 are obvious. Separate correlations between gloss and σ are obtained at 75° incidence, while no such conclusion can be drawn from the 85° data. The standard deviation is directly related to roughness, in that the larger the value of σ, the more the surface varies from a mirror surface (see Chapter II). That is, the wider the distribution of facet slopes, the rougher the surface becomes, and the more facets (or, in terms of Brush roughness, the more maxima and minima) per unit surface area are present.

Figure 14 is a plot of gloss versus facet area for the print samples. Gloss generally increased with increasing facet area. A surface with large facets produces less scattering, and thus, more specular reflection, simply because there are fewer facets per unit surface area to deflect light in a non-specular direction. As Figure 14 indicates, a single correlation curve between gloss and facet area was obtained at both 75° and 85° incidence.

These results can be summarized by stating that as facet area increases, and standard deviation decreases to zero, the surface approaches a mirror surface, and the reflectance approaches mirror reflectance.

As discussed in Chapter III, the value of facet area a was determined by matching calculated and experimental reflectance at the specular angle. Tables V and VI in Appendix B illustrate the correspondence between the calculated and experimental reflectance maxima for the print samples at 75°, and 85°, respectively. The calculated values were determined using the range of values of a obtained by matching specular reflectances. The maxima do agree, within experimental error, for many of the samples, as determined by the overlap of the experimental and calculated ranges. Thus, the theory can be

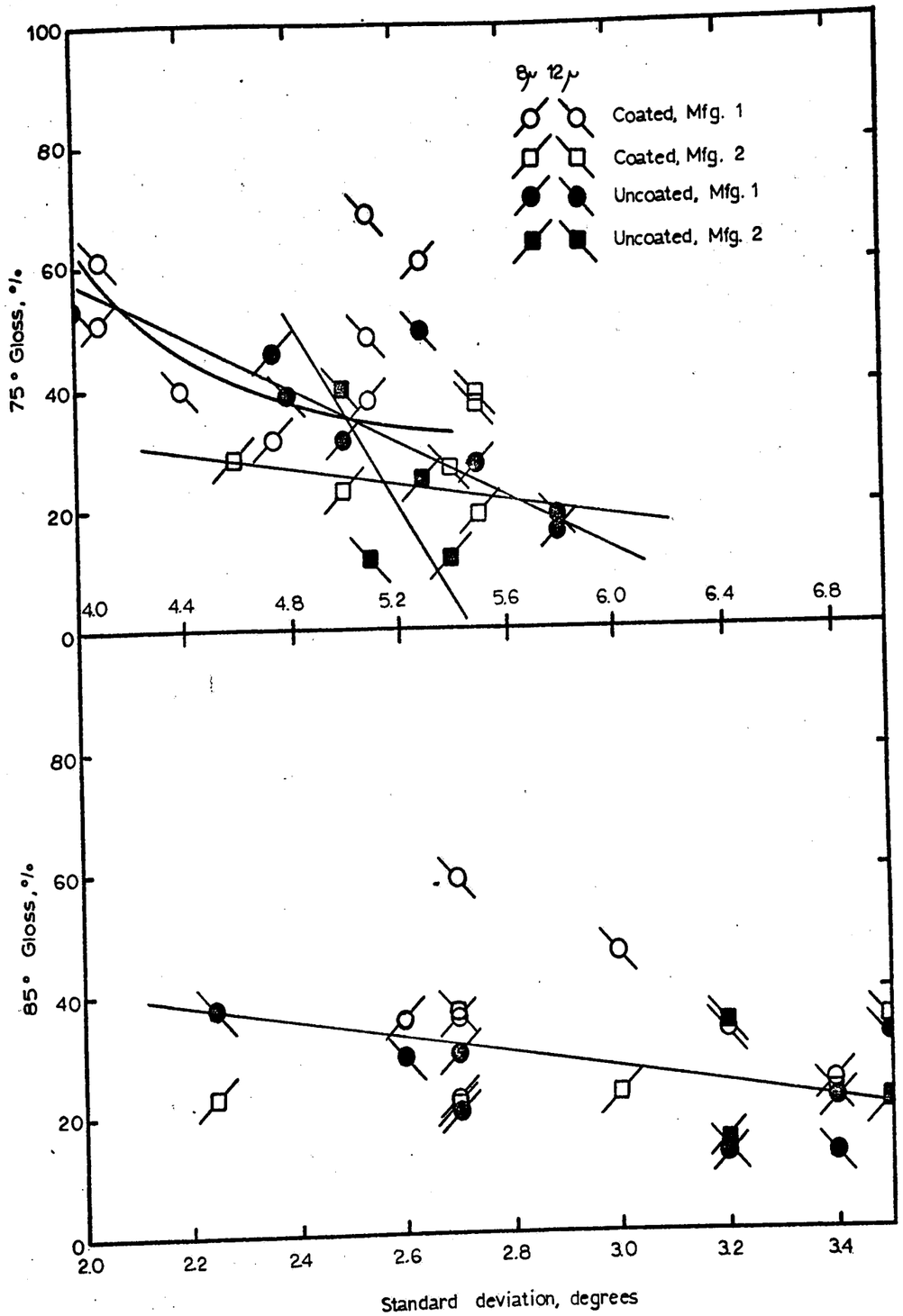

Figure 13: Gloss as a Function of Standard Deviation: 12 Mil Prints In the Machine Direction

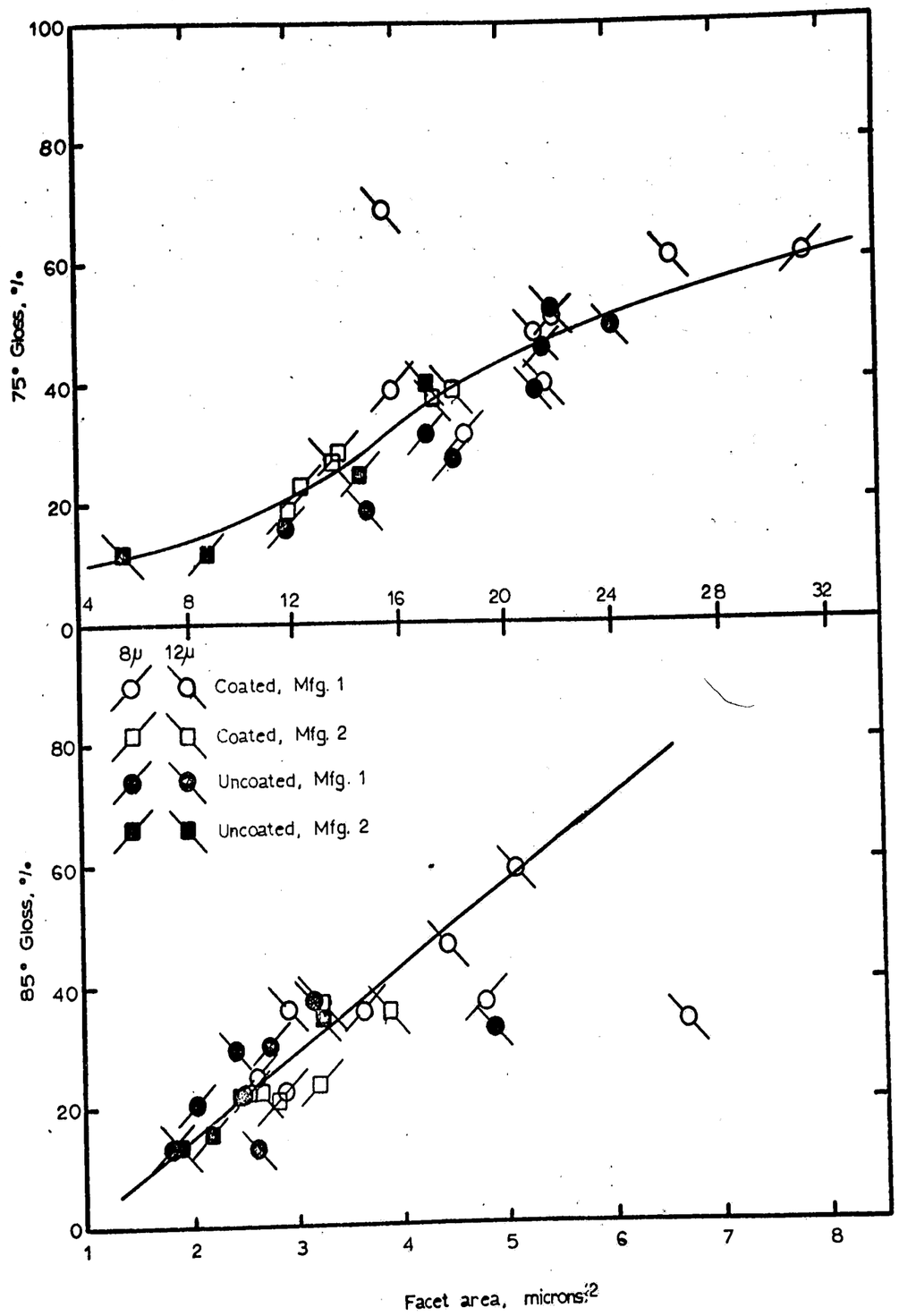

Figure 14: Gloss as a Function of Facet Area: 12 Mil Prints In the Machine Direction

made to predict the reflectance properties of these printed surfaces fairly well.

Tables VII - XII in Appendix B illustrate the results of a similar theoretical analysis of the reflectance data taken across the machine direction. In general, the values of the standard deviation were higher, and the values of the facet area were lower than those obtained for the corresponding print samples in the machine direction. The experimental curves were generally lower and wider than those in the machine direction and the reflectance maxima occurred at slightly greater angles. All of these results are to be expected, since the prints are rougher across, than they are in, the machine direction. The higher value of θ_{max}, combined with the shapes of the calculated curves, introduces a serious complication, in that for many of the rougher prints it was impossible to determine either σ or a. The correspondence between calculated and experimental reflectance maxima was not as good as that obtained in the machine direction.

In all cases, the reflectance measured by the goniophotometer was smaller than that measured by the specular glossmeter, although 85° reflectance was greater than 75° reflectance at both the specular angle and at θ_{max}. The lower goniophotometer reflectance is due to the fact that the goniophotometer employed monochromatic light, while the specular glossmeter employed white incandescent light.

V. CONCLUSIONS AND RECOMMENDATIONS

The present research was directed toward an understanding of the manner in which printed surfaces reflect light. We hoped that the reflectance properties of such surfaces could be explained in terms of meaningful physical properties of the surfaces, instead of the purely empirical, and physically meaningless, parameters generally employed in the correlation of theory and experiment for such systems. To the author's knowledge, such an approach has never been applied, in a truly rigorous manner, to printed surfaces. The results are encouraging, although significant discrepancies between theory and experiment in several areas indicate that modifications are necessary before the theoretical formulations can be considered completely successful.

The major results of the study may be summarized as follows:

a. specular reflectance decreases as the surface roughness, measured by any of several parameters, increases
b. maximum reflectance occurs at a viewing angle which is somewhat larger than the specular angle, due to Fresnel reflectance overemphasizing those facets with slopes greater than zero
c. the geometry of illumination and viewing can drastically affect the reflectance properties of prints, especially glossy prints
d. the reflectance model, as developed here is a simplified form with two adjustable surface parameters, can be made to fit the experimental reflectance data adequately, but the parameter values obtained are not realistic, since the values calculated at two different incident angles do not agree within experimental error.

The discrepancies between theory and experiment are the result of certain idealizations in the model, which is similar to several models which have been applied, with some success, to surfaces such as ground glass and roughened metal. Such surfaces, which generally are prepared by grinding with a uniform abrasive, are composed of small, irregular chips which approximate small, specularly reflecting facets. A board surface, however, is composed of fibers which are generally irregular in their shape and alignment. It is to be expected that the surface of a print will, to some degree, reflect the configuration of the substrate on which it is formed. Thus, the surface of a print may be significantly different from that of ground glass or similar surfaces, and the assumption of small facets of equal areas forming symmetric V-groove cavities whose slopes are distributed according to the normal distribution is open to considerable question. Until a method is found for studying the surface configuration of printed materials directly, the present theory cannot be made completely rigorous.

The author believes that this can, and should, be done. The continued development and improvement of such methods of surface study as scanning electron microscopy may be of great value in the determination of surface configuration. Once such a method has been realized it will be possible to determine, in advance, and to a high degree of accuracy, the reflectance properties of any print-substrate combination.

In the meantime several steps can be taken to improve the present theory. It is possible that a distribution other than the normal distribution may more adequately describe the facet orientations. The elimination of the assumption of symmetric V-groove cavities with longitudinal axes parallel to the plane of the mean surface and with the upper edges all lying in the same plane may increase the model accuracy, although this would complicate the

development of the geometrical attenuation factor.

As has been previously mentioned, the instrument employed in the experimental work was not originally designed for this purpose, and several problems arose from this fact. The method of determination of incident and viewing angles was not sufficiently accurate, and the angular resolution of the receptor was not acceptable. In view of these equipment shortcomings, the accuracy obtained is perhaps as good as can be expected.

APPENDIX

A. Experimental Reflectance Curves

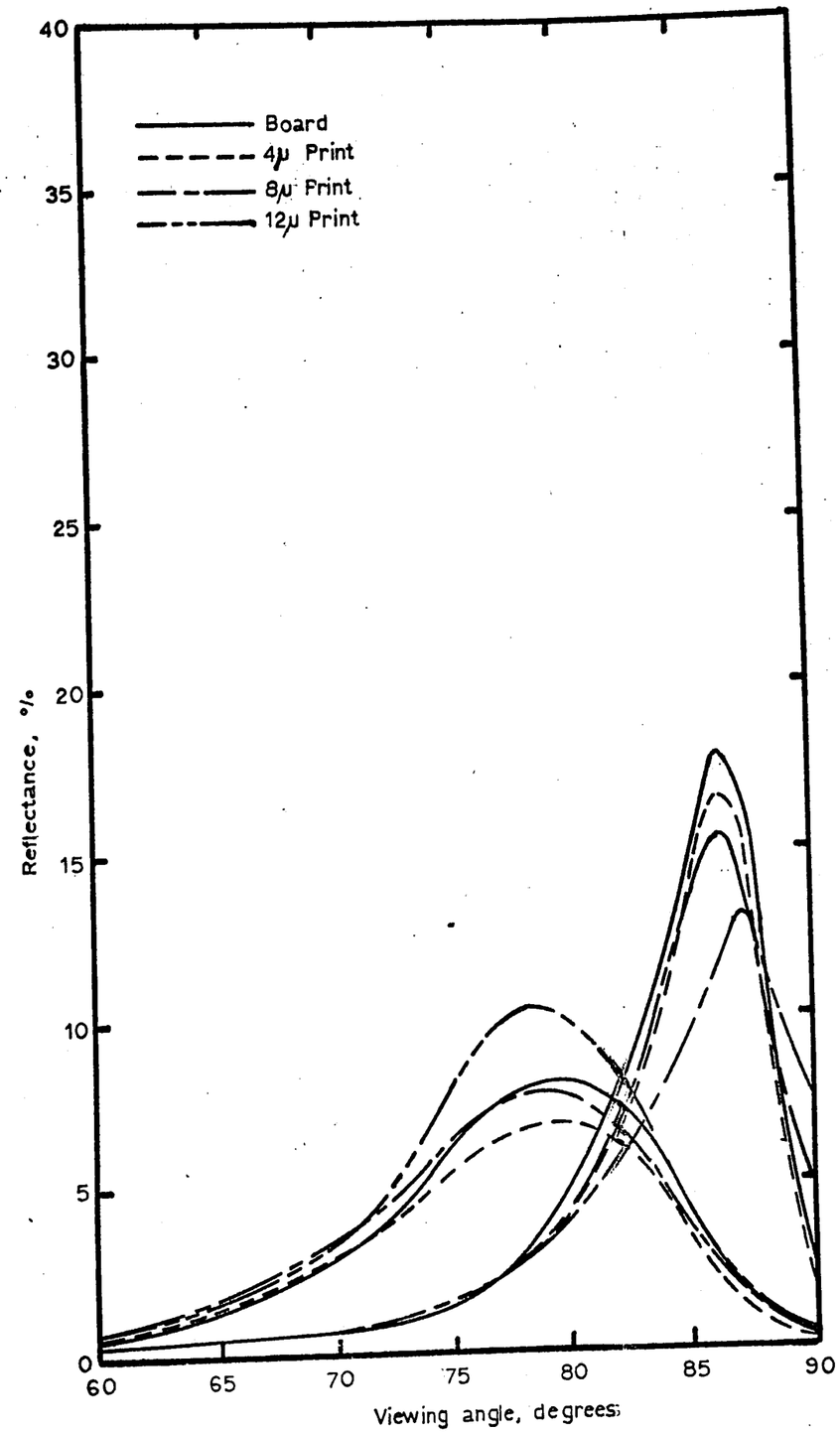

Figure A1: A1-0485 In Machine Direction

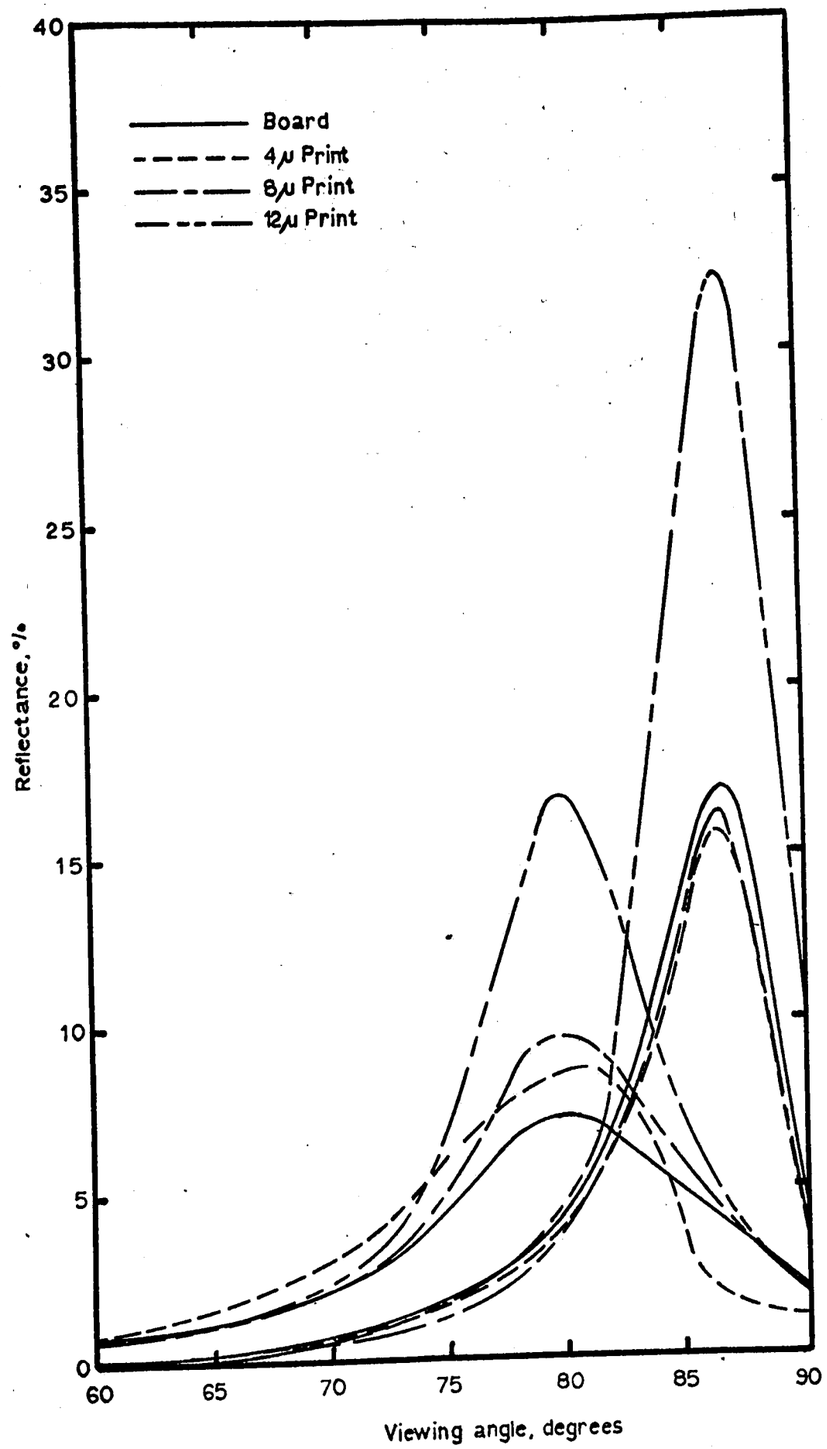

Figure A2: A2-0189 In Machine Direction

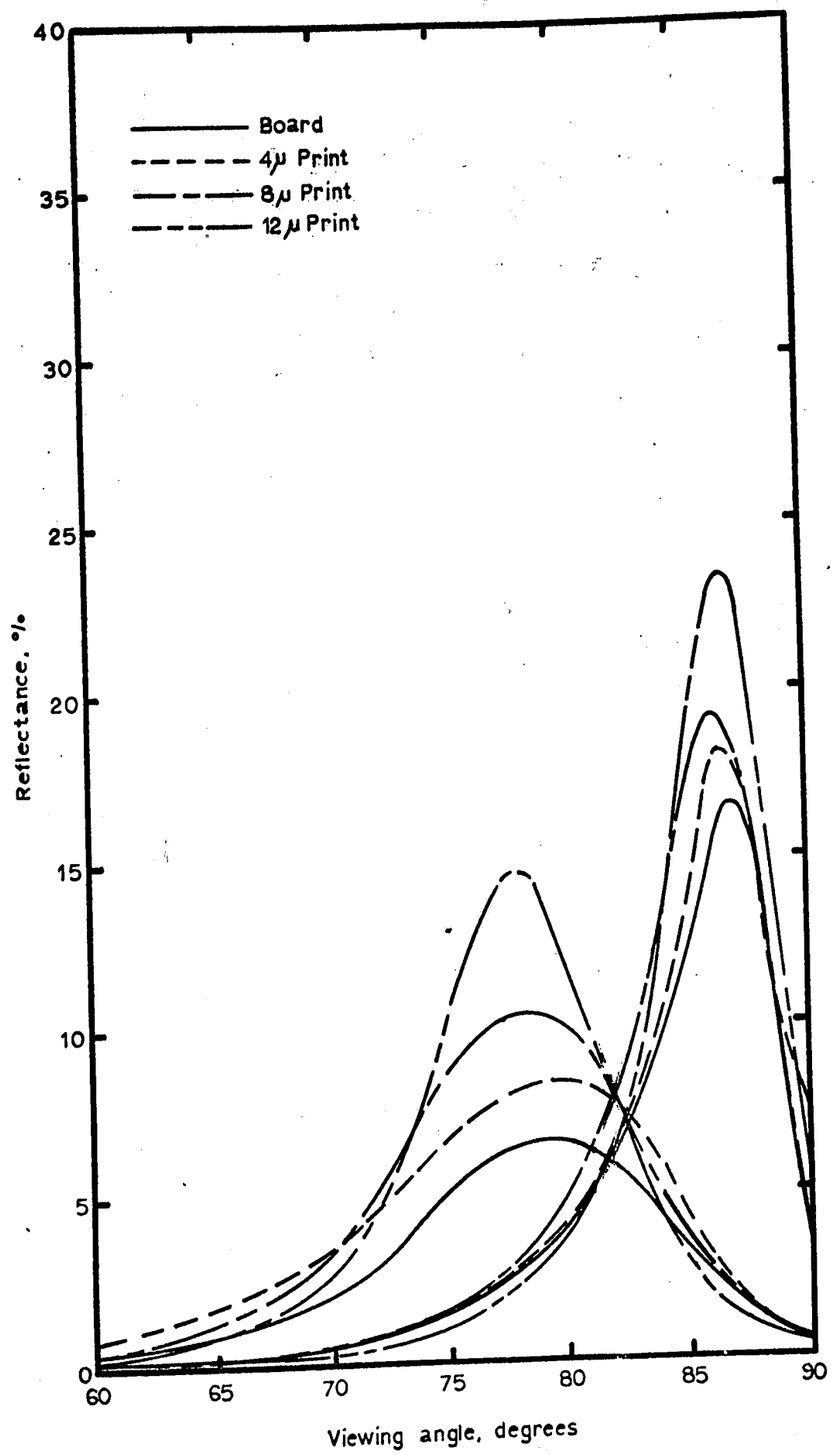

Figure A3: A3-0248 In Machine Direction

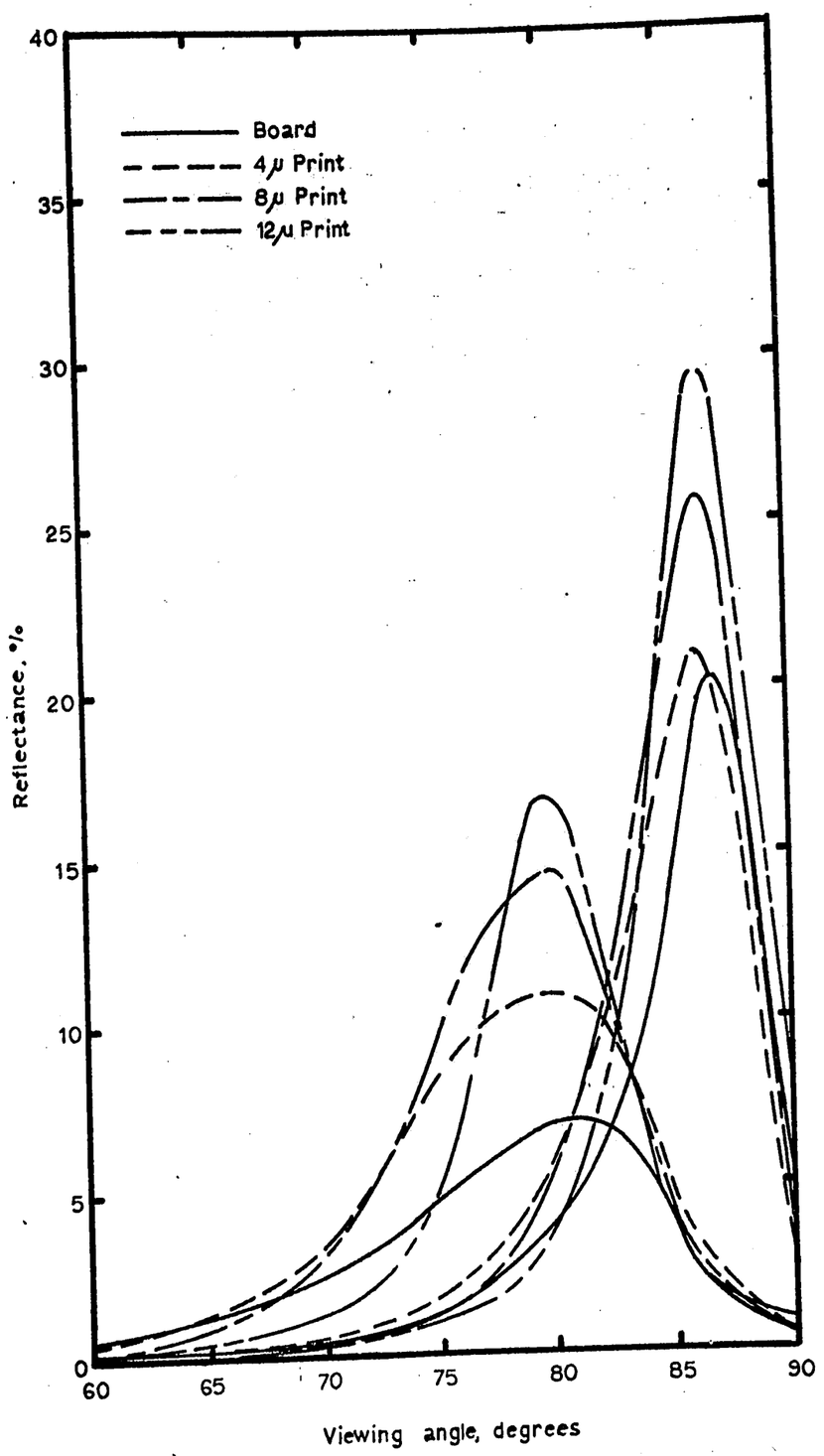

Figure A4: A4-0750 In Machine Direction

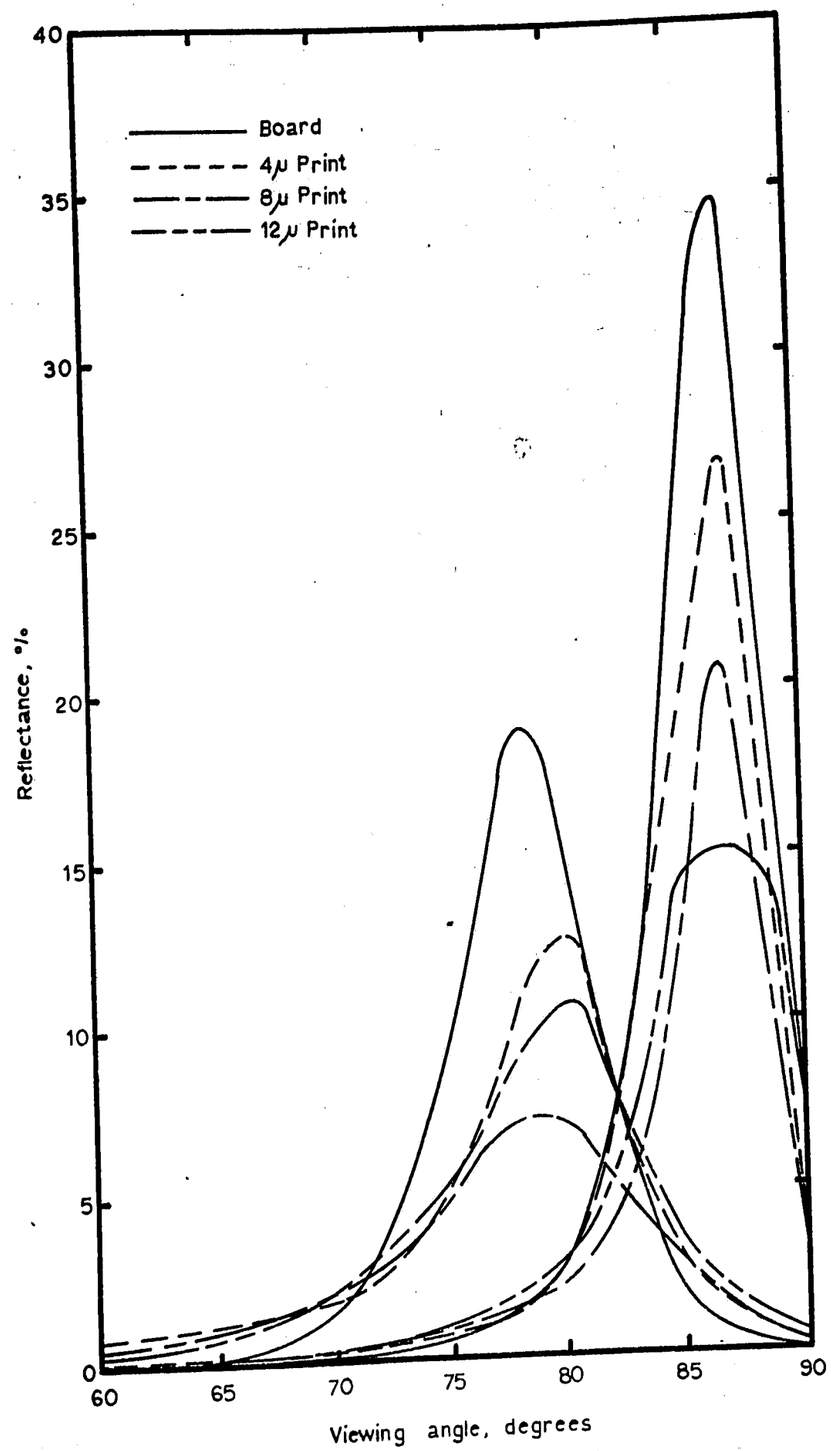

Figure A5: A5-0604 In Machine Direction

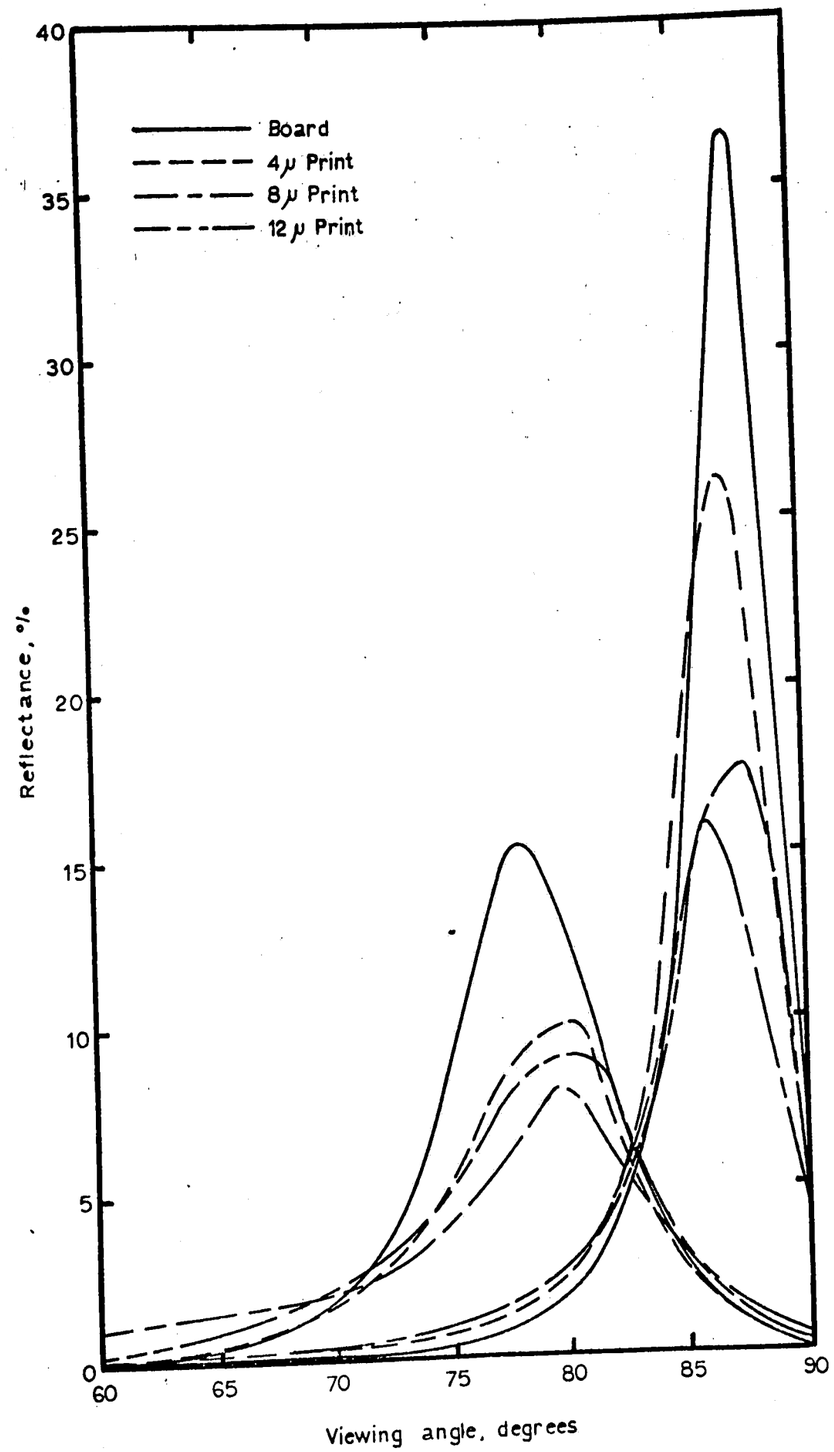

Figure A6: A6-0648 In Machine Direction

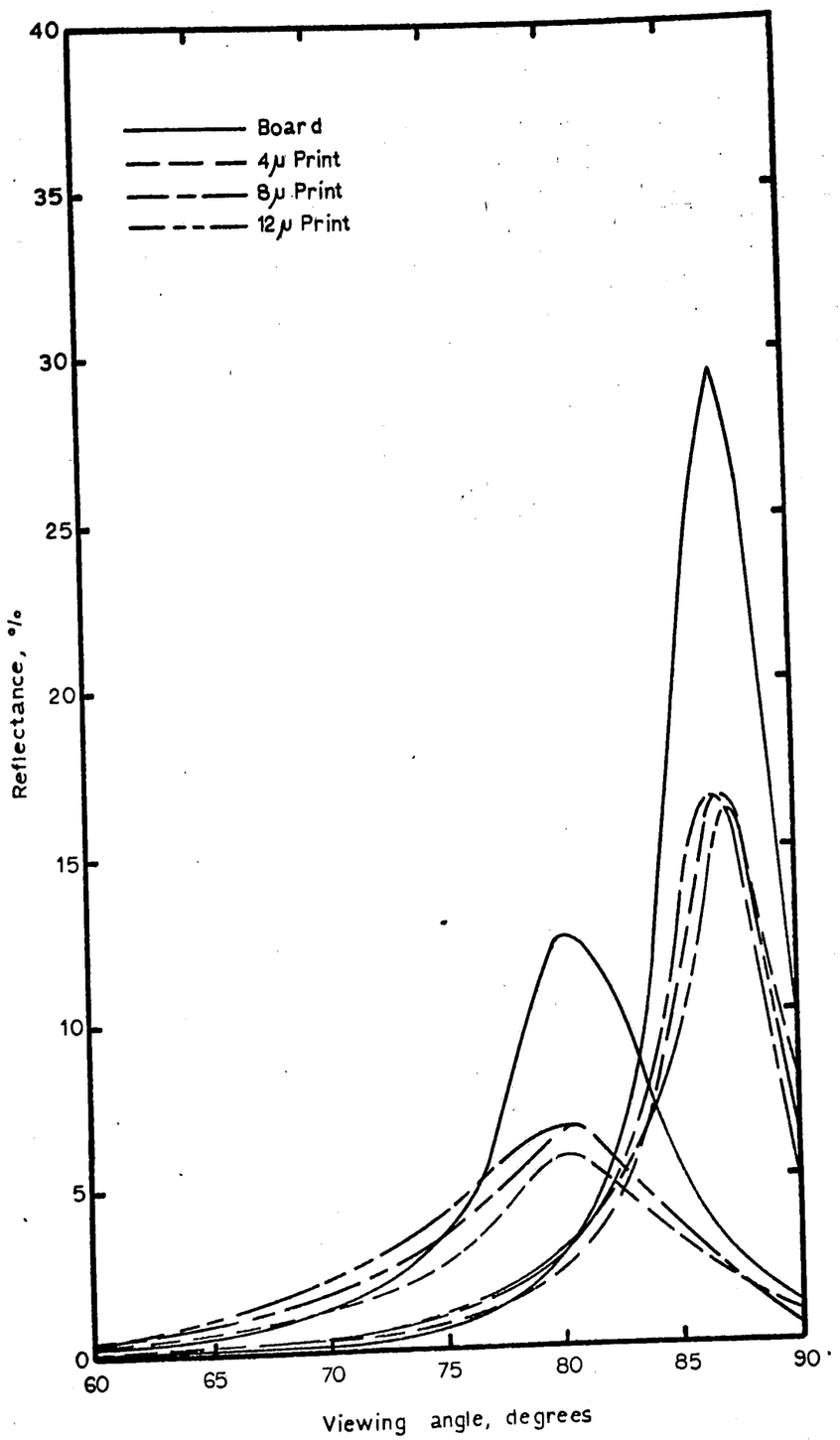

Figure A7: A7-0009 In Machine Direction

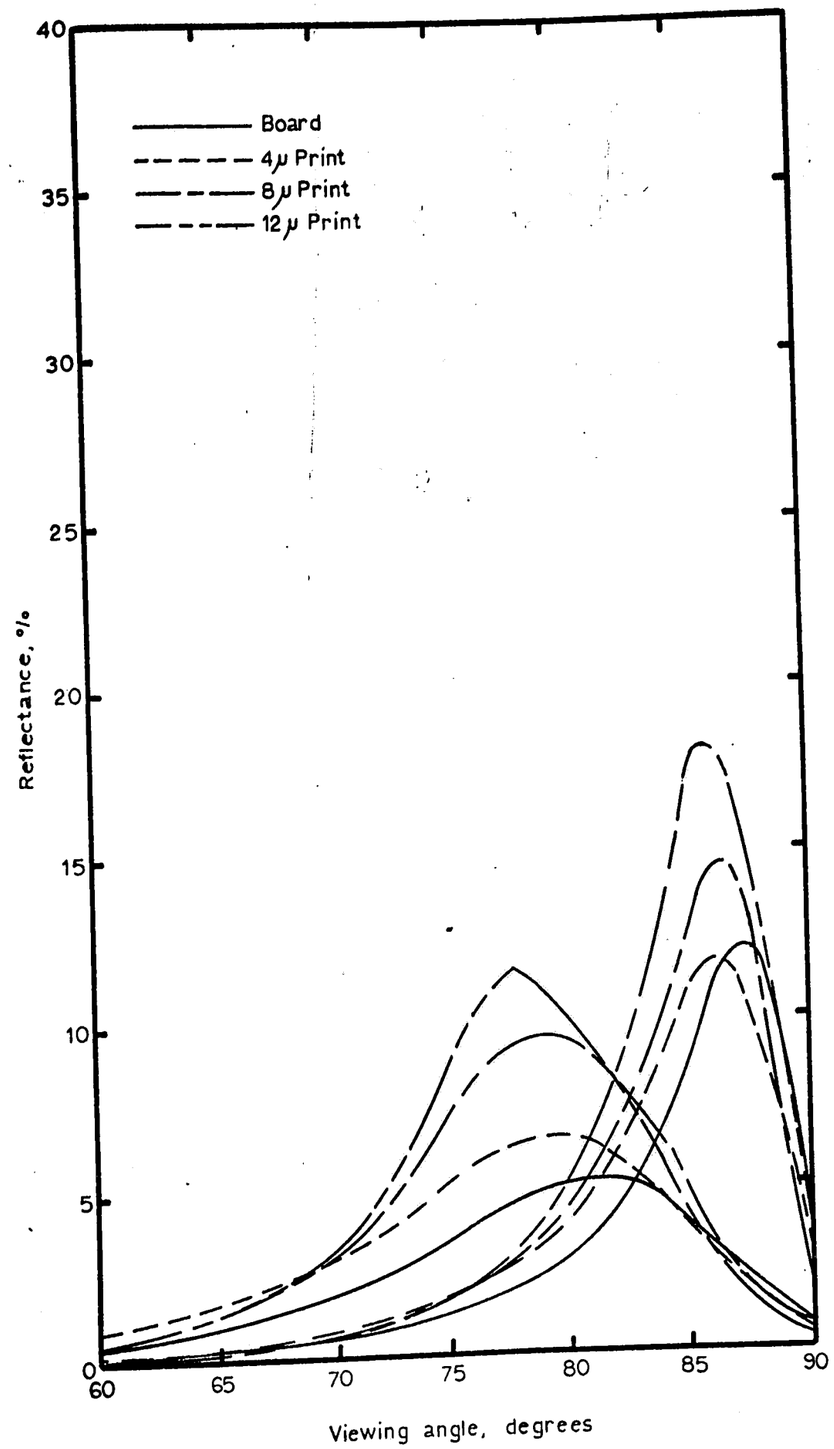

Figure A8: B1-0228 In Machine Direction

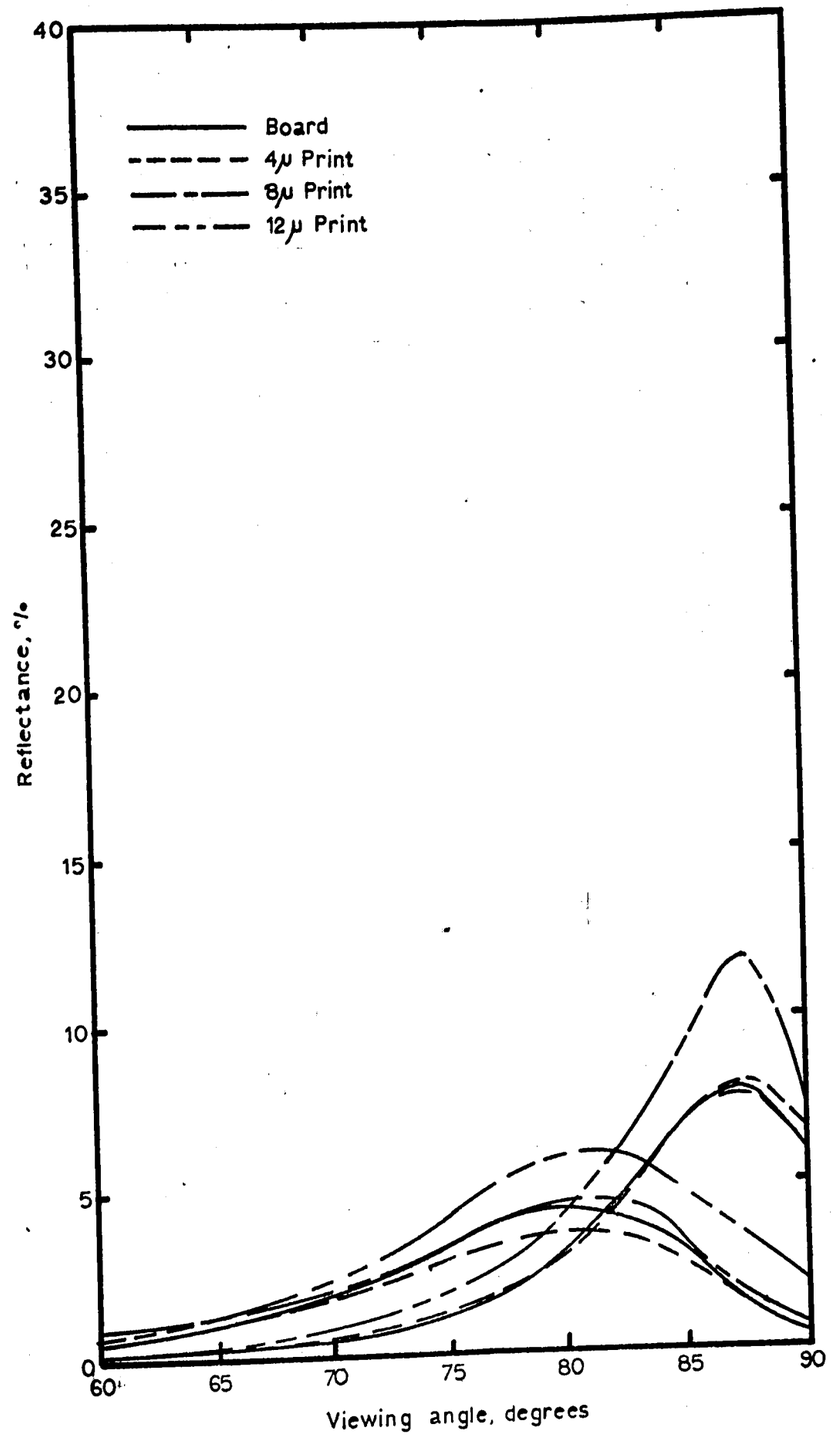

Figure A9: B2-1369 In Machine Direction

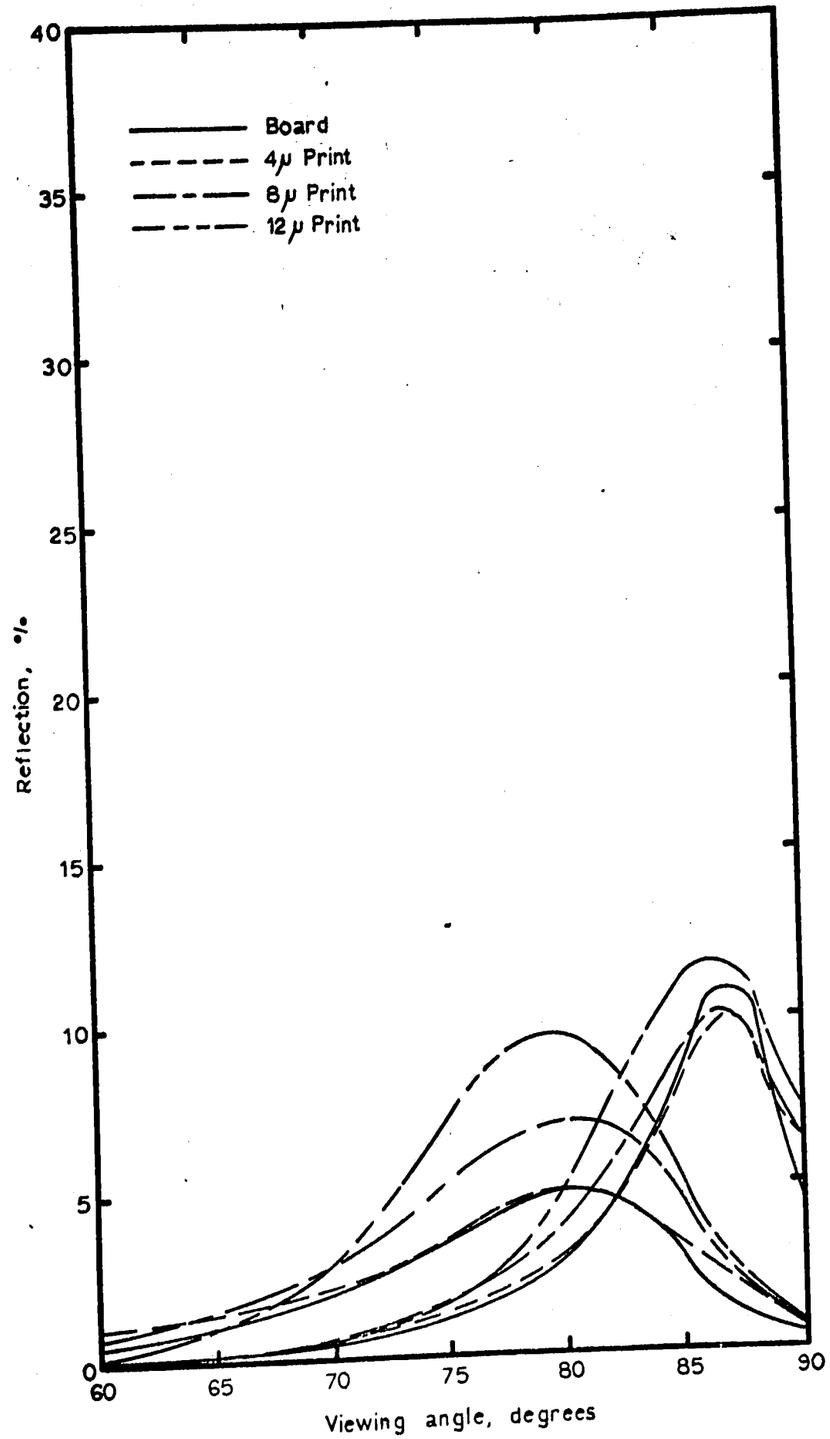

Figure A10: B3-0185 In Machine Direction

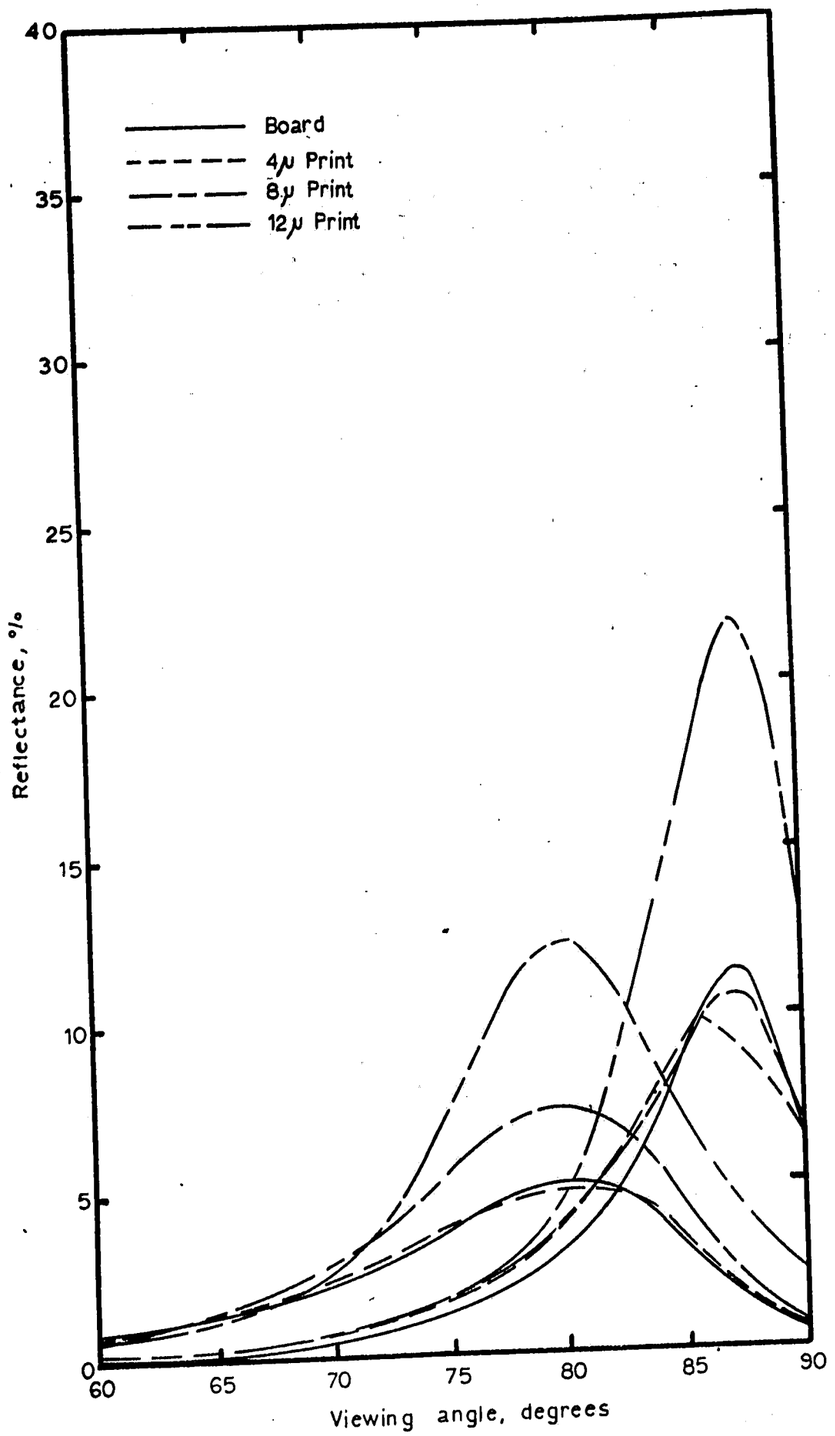

Figure A11: B4-0943 In Machine Direction

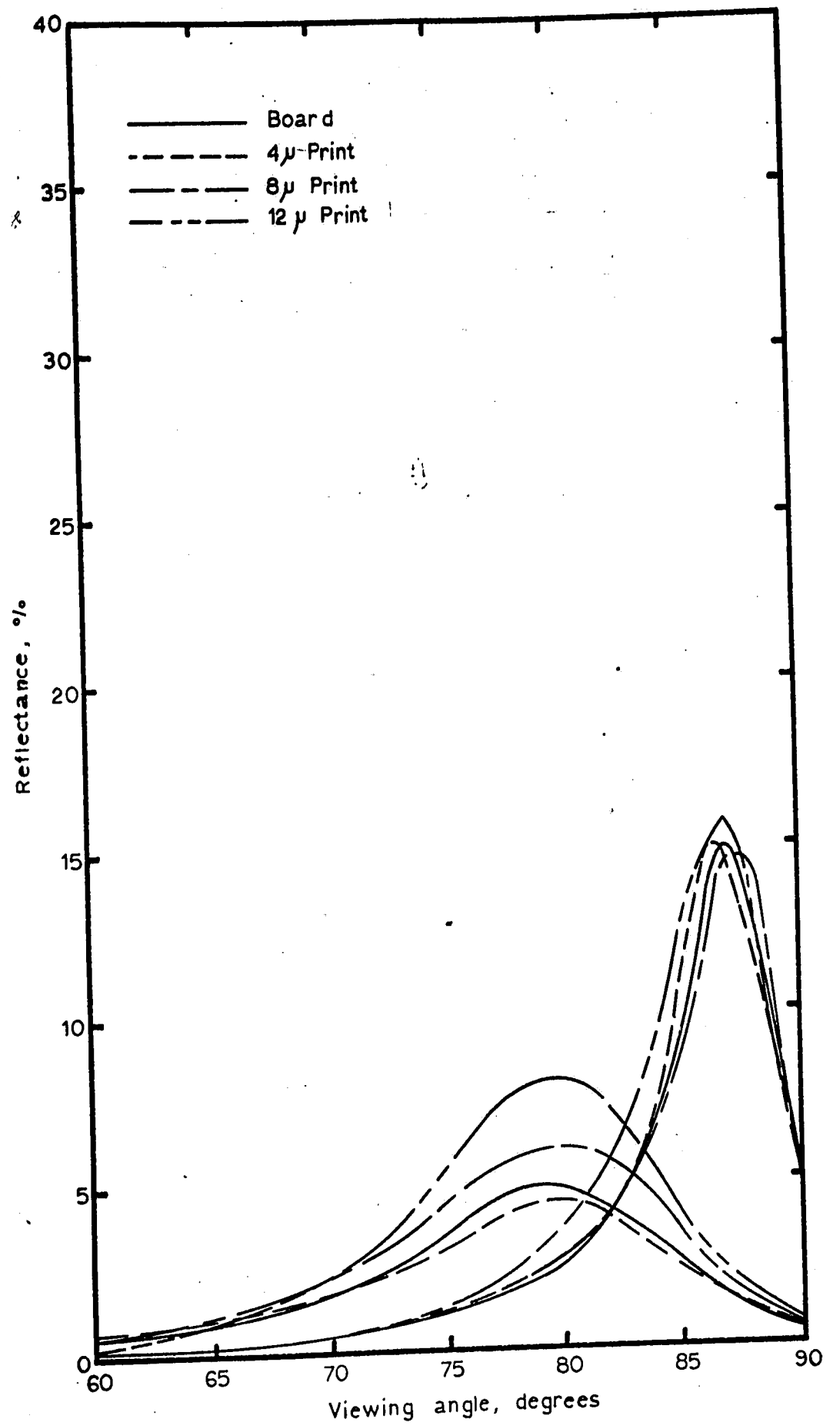

Figure A12: B5-0514 In Machine Direction

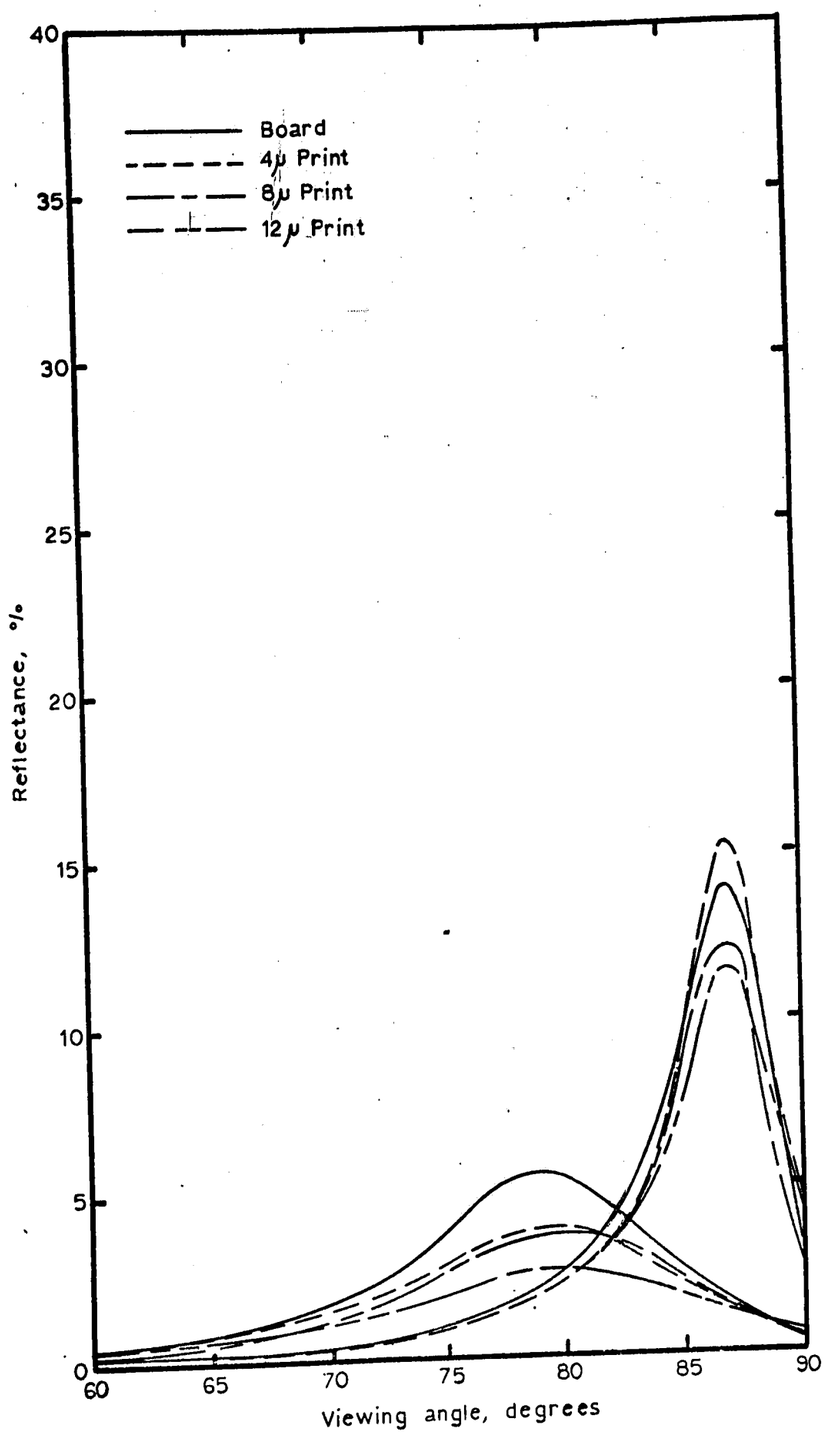

Figure A13: B6-0878 In Machine Direction

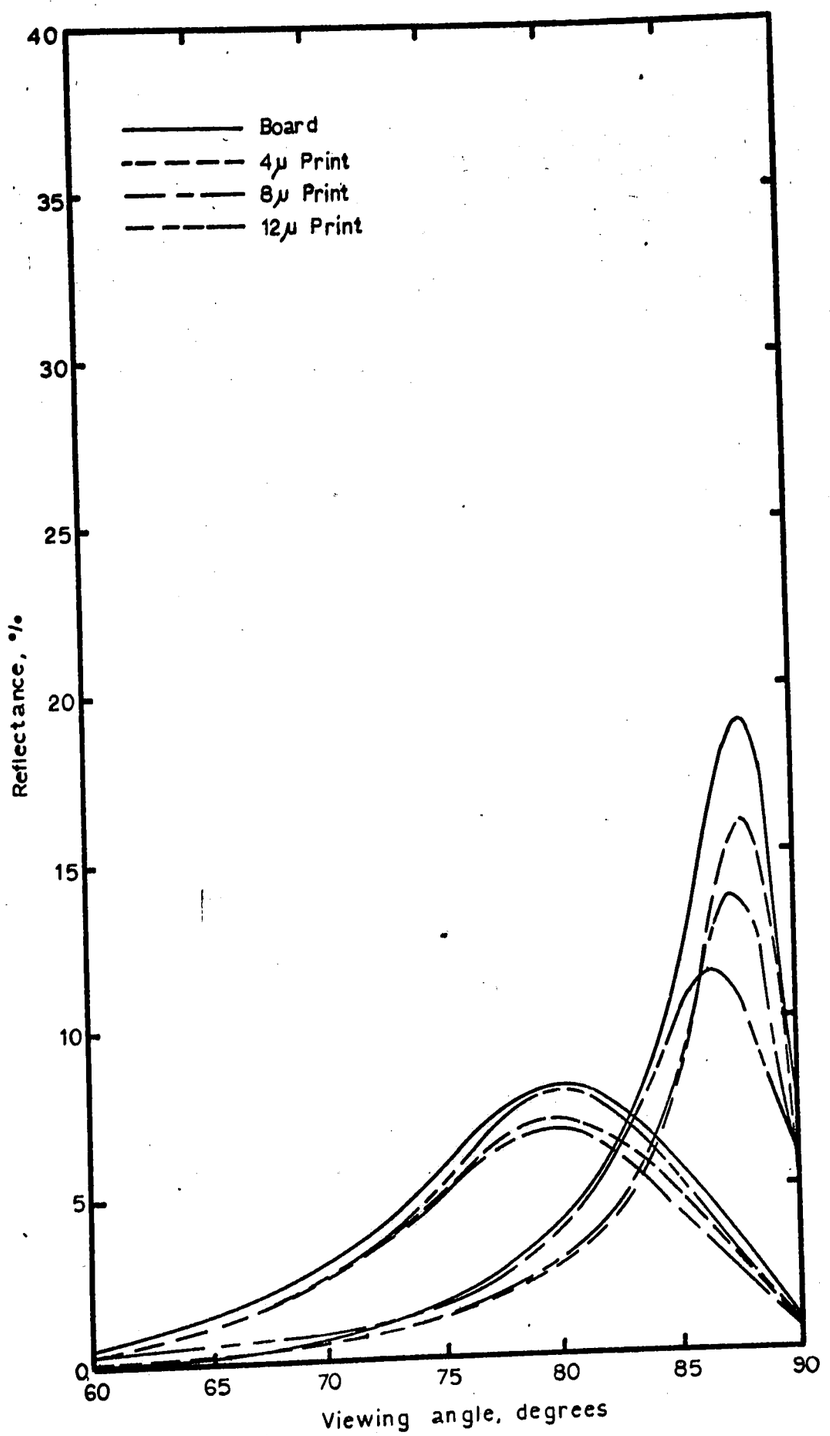

Figure A14: A1-0485 Across Machine Direction

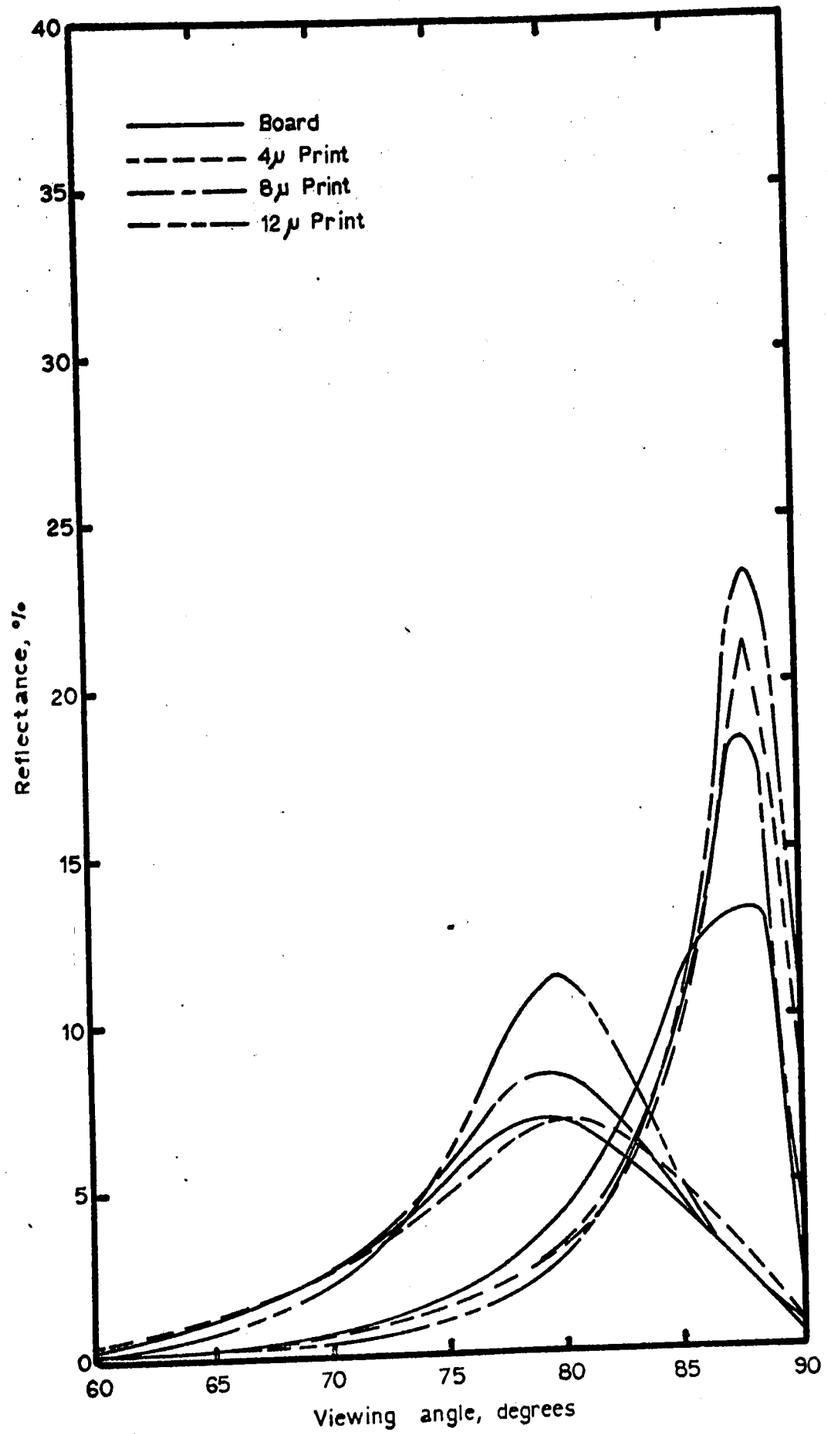

Figure A15: A2-0189 Across Machine Direction

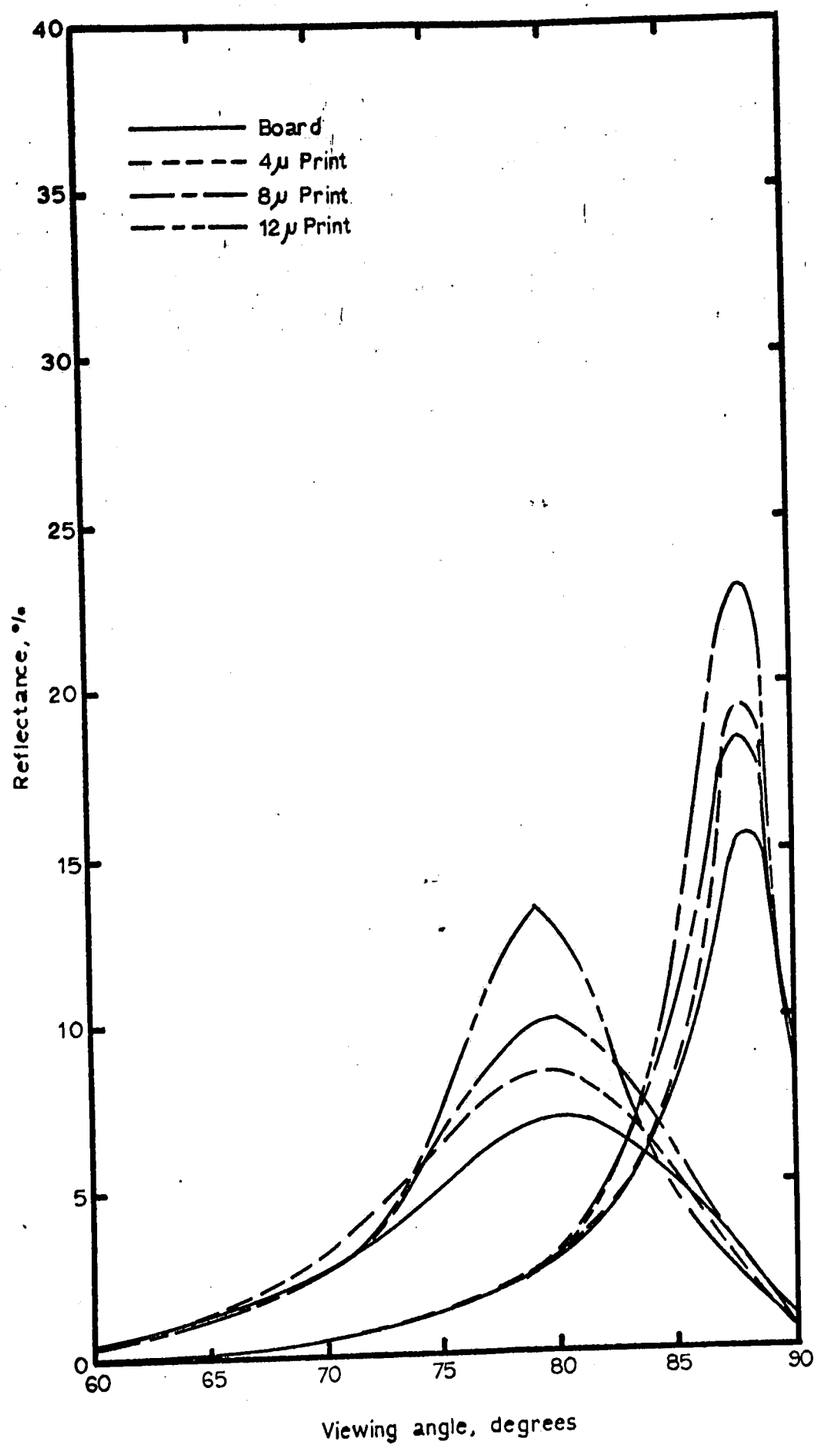

Figure A16: A3-0248 Across Machine Direction

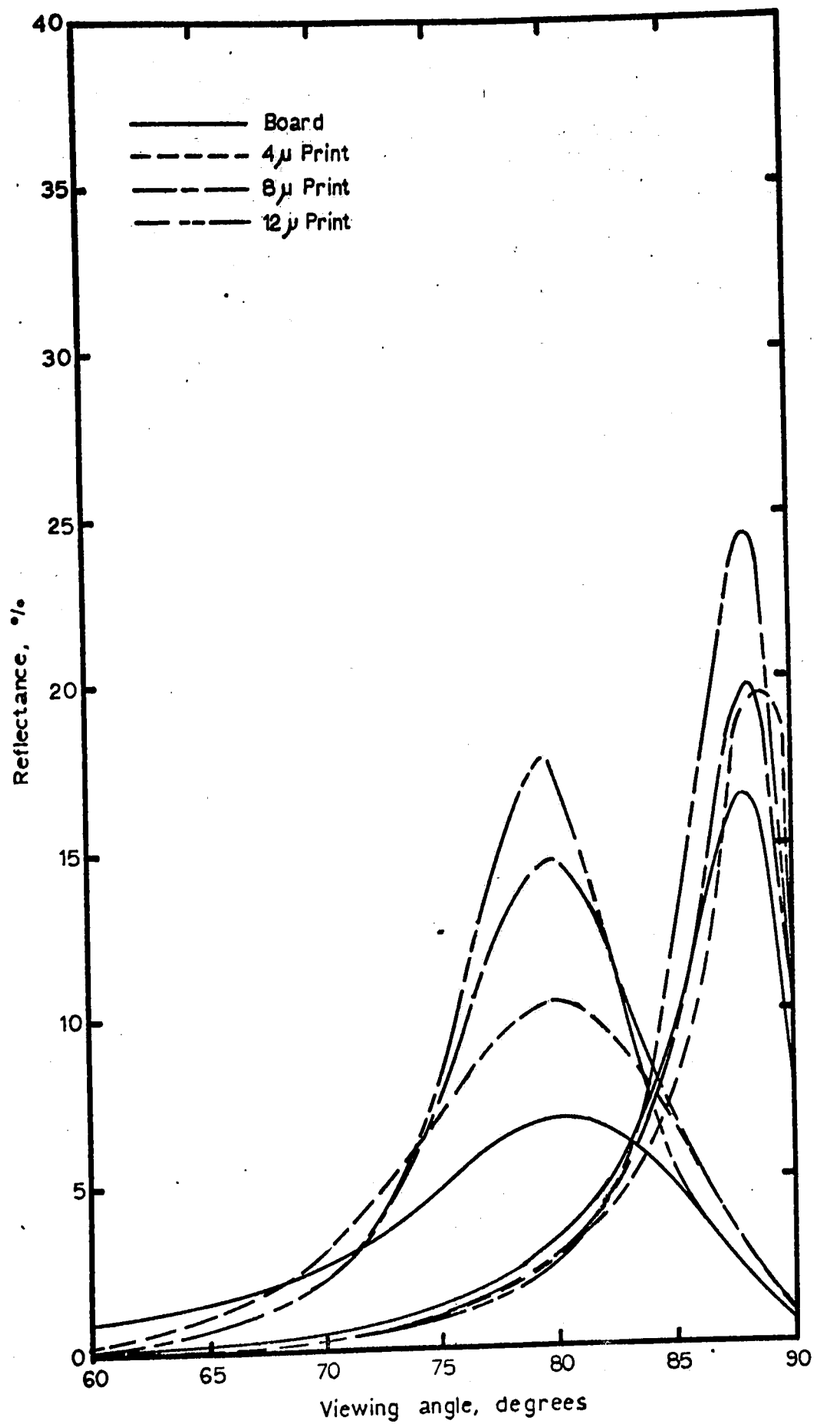

Figure A17: A4-0750 Across Machine Direction

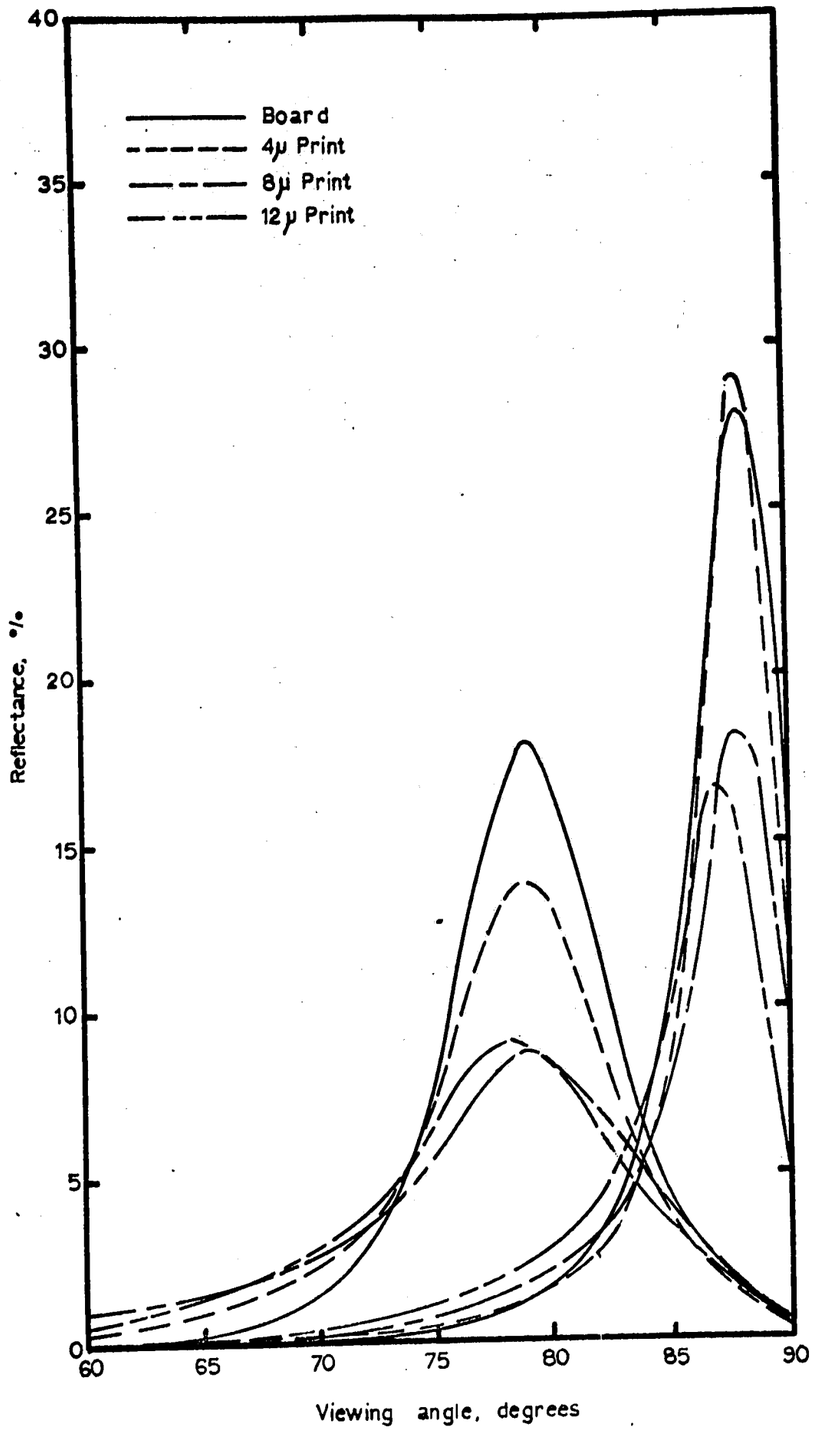

Figure A18: A5-0604 Across Machine Direction

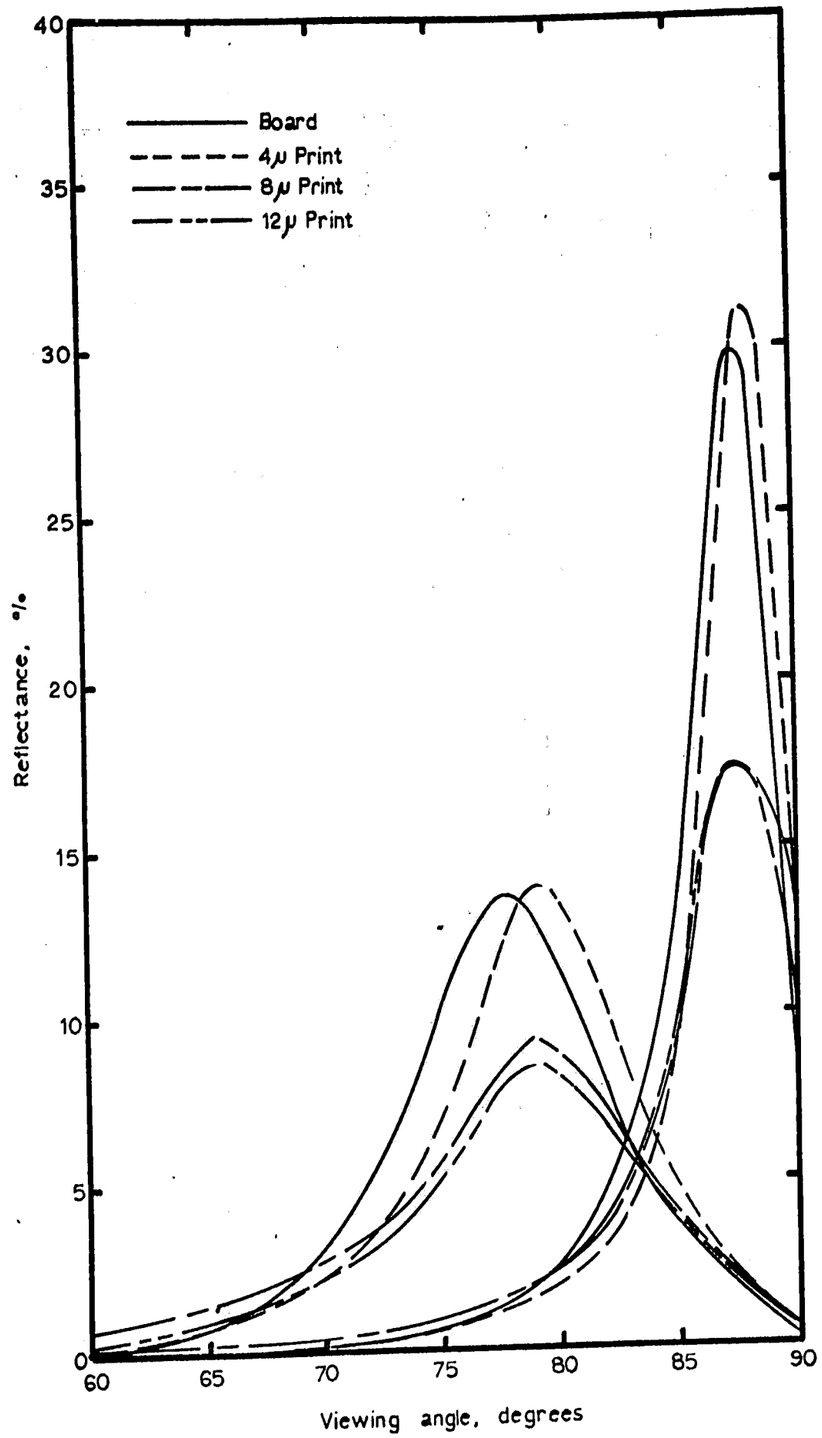

Figure A19: A6-0648 Across Machine Direction

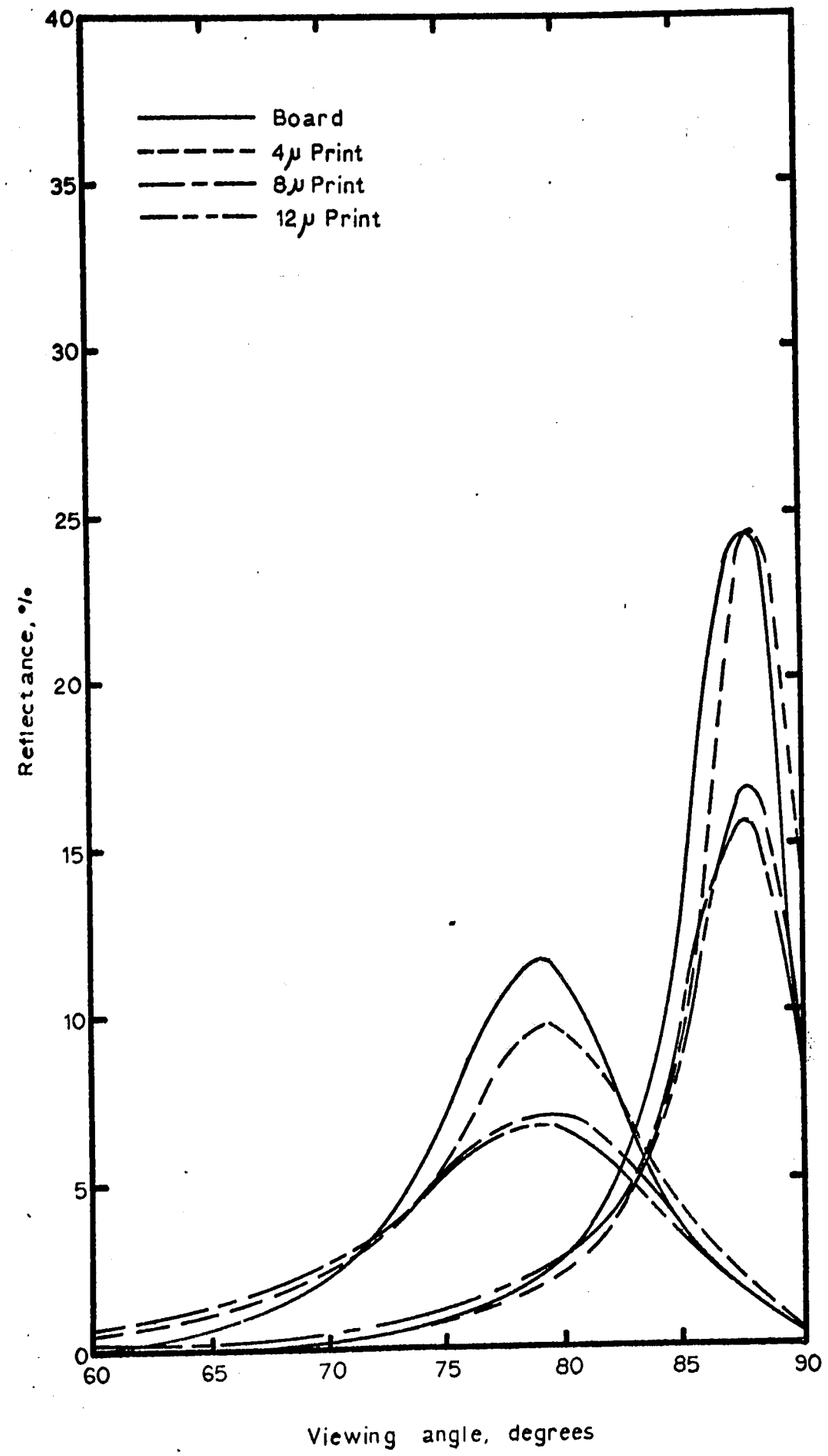

Figure A20: A7-0009 Across Machine Direction

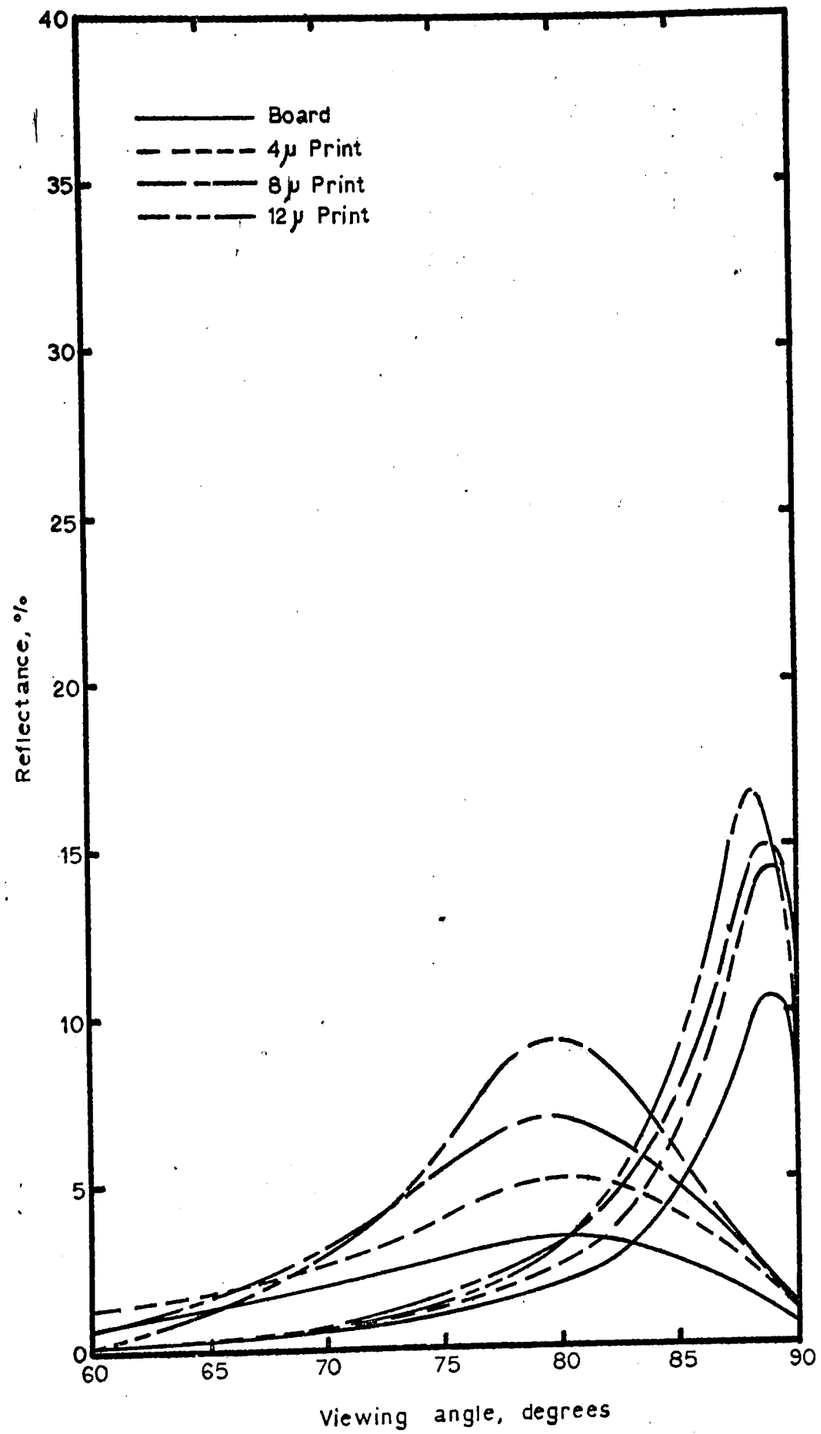

Figure A21: B1-0228 Across Machine Direction

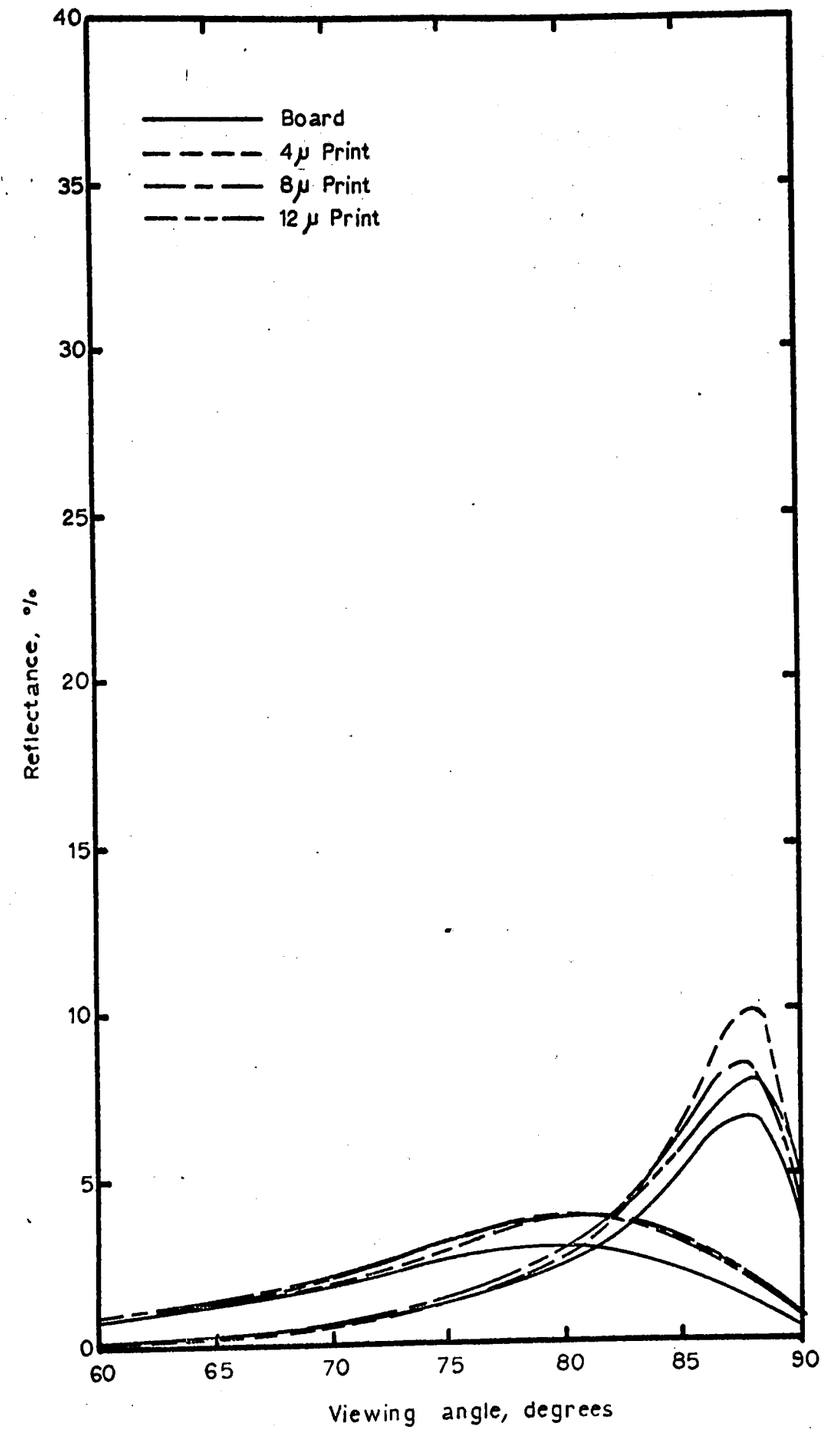

Figure A22: B2-1369 Across Machine Direction

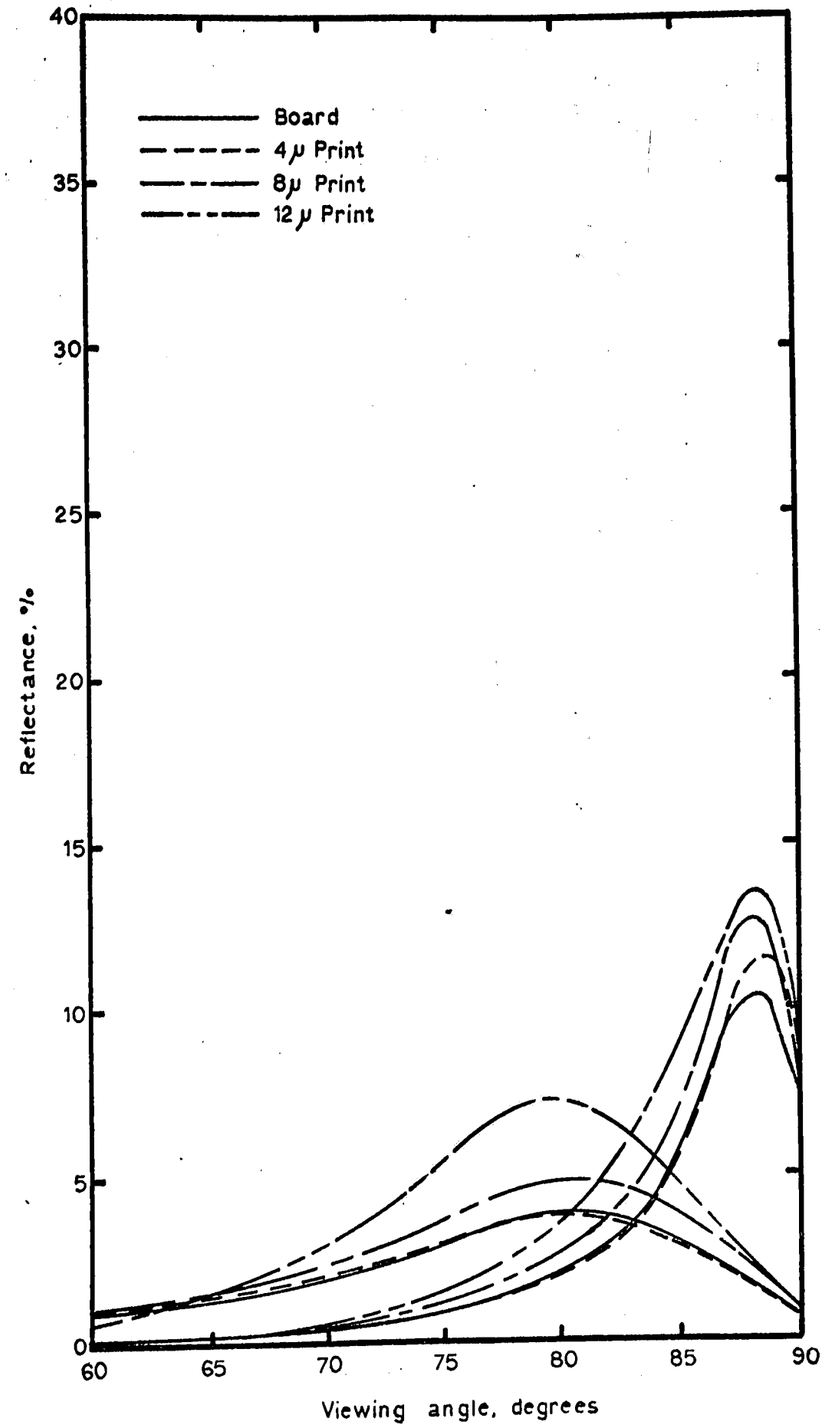

Figure A23: B3-0185 Across Machine Direction

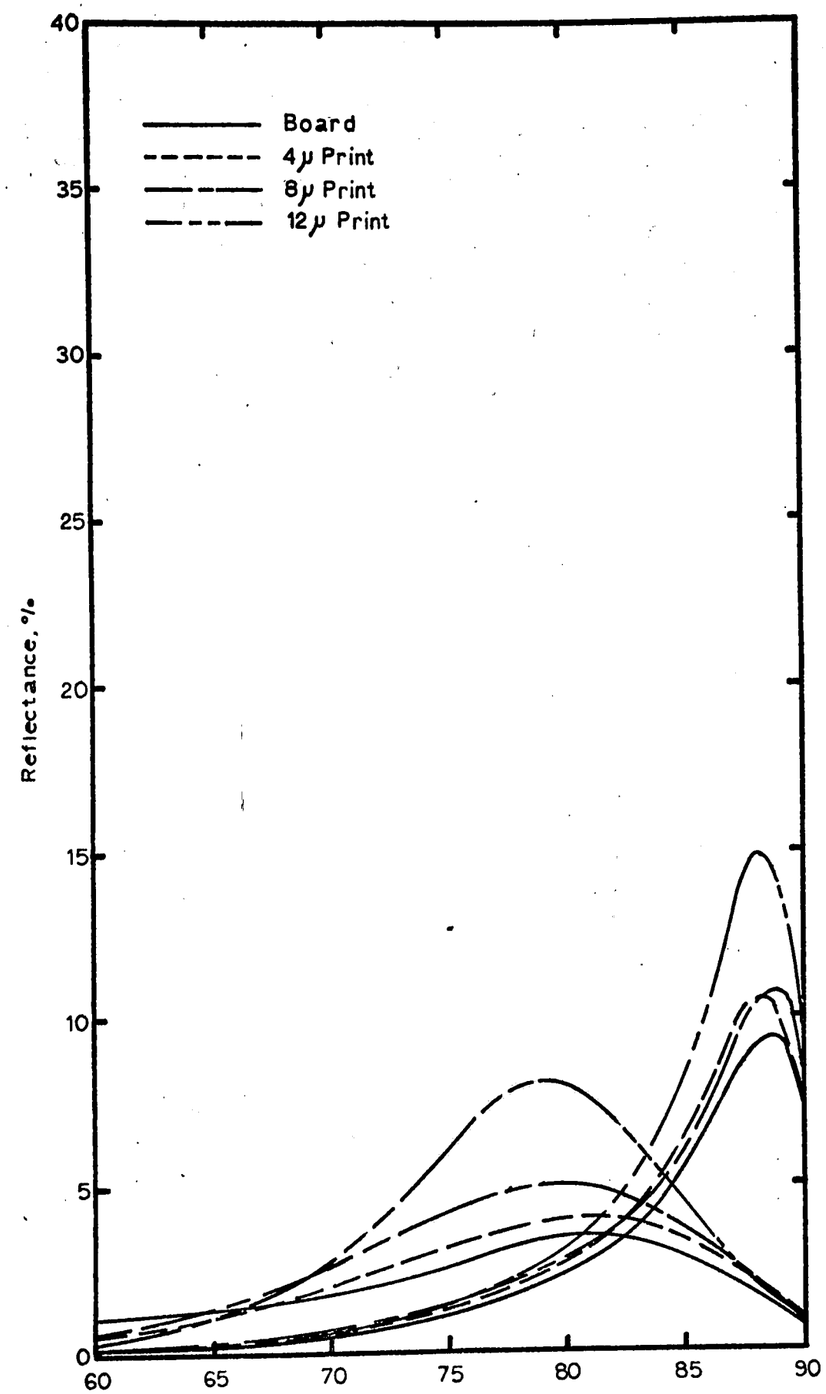

Figure A24: B4-0943 Across Machine Direction

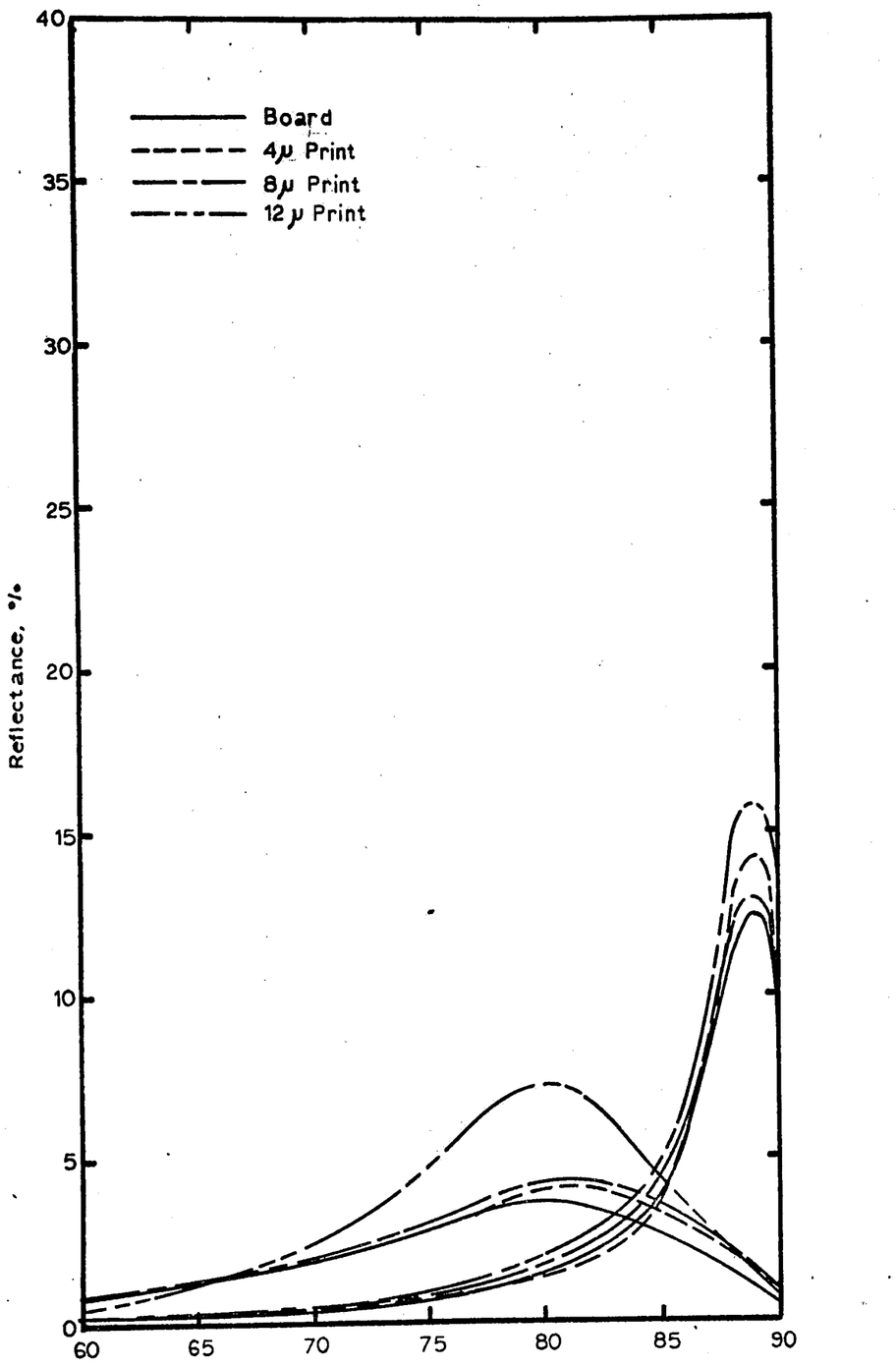

Figure A25: B5-0514 Across Machine Direction

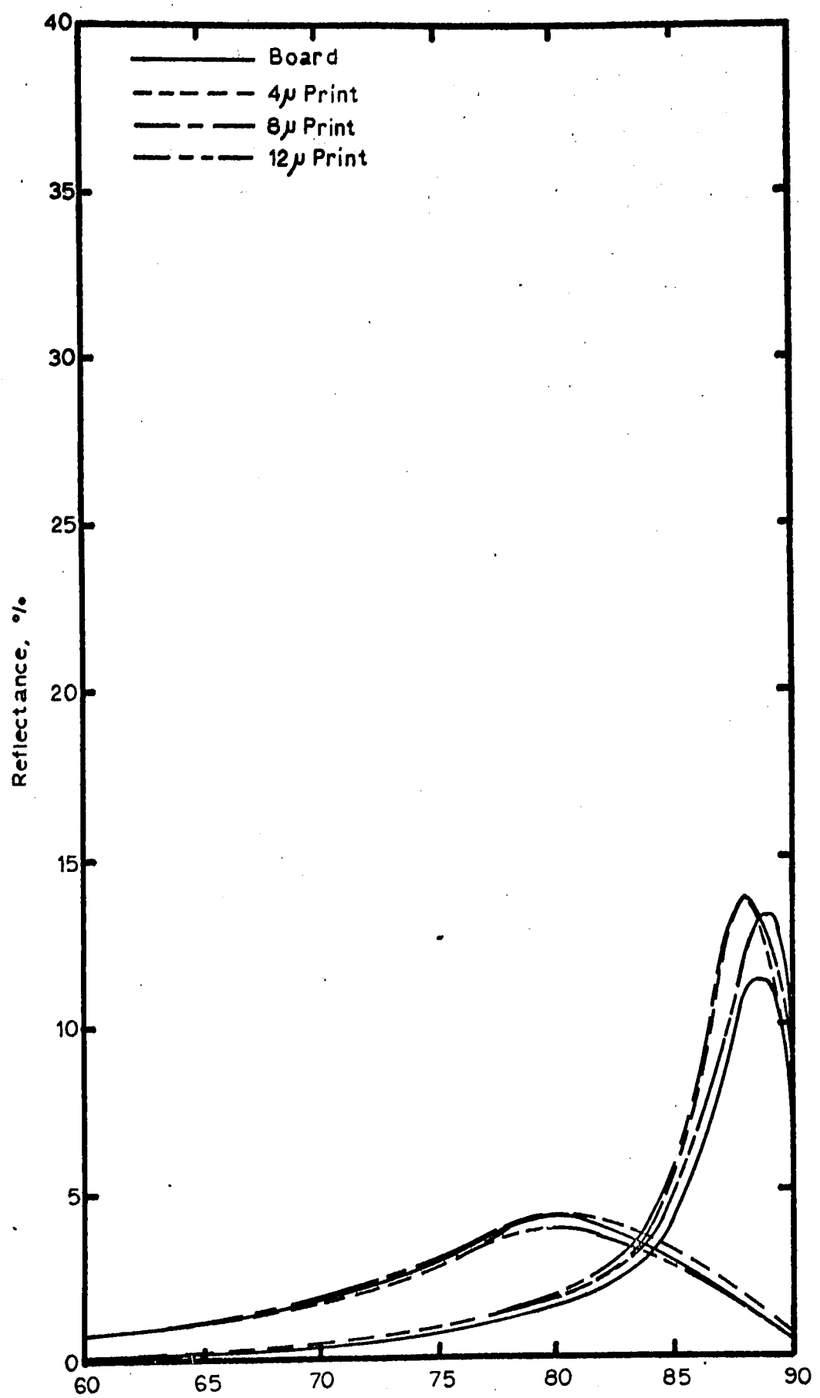

Figure A26: B6-0878 Across Machine Direction

B. Comparison of Experimental and Theoretical Reflectance Data

Table I: Position of Reflectance Maximum, θ_{max}, and Value and Range of Standard Deviation, σ, for Print Samples at 75° Incidence, In the Machine Direction

Board	Print	θ_{max} deg.	σ, deg.	σ range, deg.
		Coated Boards		
A1-0485	8 μ	79.0	4.75	4.10-5.30
	12 μ	78.5	4.40	3.80-5.00
A2-0189	8 μ	79.75	5.10	4.60-5.70
	12 μ	79.75	5.10	4.60-5.70
A3-0248	8 μ	78.0	4.10	3.40-4.75
	12 μ	78.0	4.10	3.40-4.75
A4-0750	8 μ	80.0	5.30	4.75-5.80
	12 μ	79.75	5.10	4.60-5.70
A5-0604	8 μ	78.75	4.60	3.90-5.10
	12 μ	80.5	5.50	5.00-6.00
A6-0648	8 μ	79.5	5.00	4.40-5.50
	12 μ	80.5	5.50	5.00-6.00
A7-0009	8 μ	80.5	5.50	5.00-6.00
	12 μ	80.25	5.40	4.80-5.90
		Uncoated Boards		
B1-0228	8 μ	79.0	4.75	4.10-5.30
	12 μ	77.75	4.00	3.20-4.60
B2-1369	8 μ	81.0	5.80	5.30-6.20
	12 μ	81.0	5.80	5.30-6.20
B3-0185	8 μ	80.5	5.50	5.00-6.00
	12 μ	79.25	4.80	4.25-5.40
B4-0943	8 μ	79.5	5.00	4.40-5.50
	12 μ	80.0	5.30	4.75-5.80
B5-0514	8 μ	80.0	5.30	4.75-5.80
	12 μ	79.5	5.00	4.40-5.50
B6-0878	8 μ	80.25	5.40	4.80-5.90
	12 μ	79.75	5.10	4.60-5.70

Table II: Position of Reflectance Maximum, θ_{max}, and Value and Range of Standard Deviation, σ, for Print Samples at 85° Incidence, In the Machine Direction

Board	Print	θ_{max}, deg.	σ, deg.	σ range, deg.
		Coated Boards		
A1-0485	8μ	87.25	3.40	2.60-
	12μ	86.5	2.70	1.60-3.55
A2-0189	8μ	86.5	2.70	1.60-3.55
	12μ	87.0	3.20	2.25-
A3-0248	8μ	86.25	2.60	1.20-3.40
	12μ	86.75	3.00	2.00-3.70
A4-0750	8μ	86.5	2.70	1.60-3.55
	12μ	86.5	2.70	1.60-3.55
A5-0604	8μ	86.75	3.00	2.00-3.70
	12μ	86.5	2.70	1.60-3.55
A6-0648	8μ	86.0	2.25	0 -3.20
	12μ	87.5	3.55	2.70-
A7-0009	8μ	86.5	2.70	1.60-3.55
	12μ	87.25	3.40	2.60-
		Uncoated Boards		
B1-0228	8μ	86.5	2.70	1.60-3.55
	12μ	86.0	2.25	0 -3.20
B2-1369	8μ	87.0	3.20	2.25-
	12μ	87.25	3.40	2.60-
B3-0185	8μ	86.5	2.70	1.60-3.55
	12μ	86.25	2.60	1.20-3.40
B4-0943	8μ	87.25	3.40	2.60-
	12μ	87.5	3.55	2.70-
B5-0514	8μ	87.5	3.55	2.70-
	12μ	87.0	3.20	2.25-
B6-0878	8μ	87.0	3.20	2.25-
	12μ	87.0	3.20	2.25-

Table III: Specular Reflectance, ρ_{spec}, and Value and Range of Facet Area, a, for Print Samples at 75° Incidence, In the Machine Direction

Board	Print	ρ_{spec}, %	a, μ^2	a range, μ^2
		Coated Boards		
A1-0485	8μ	6.3	37.4	33.8-40.8
	12μ	7.9	43.4	39.0-47.8
A2-0189	8μ	5.0	31.8	28.6-35.0
	12μ	6.7	42.6	38.1-47.2
A3-0248	8μ	8.6	44.0	39.4-48.8
	12μ	10.3	52.8	47.6-58.0
A4-0750	8μ	9.5	62.8	56.2-69.6
	12μ	4.9	31.2	28.0-34.4
A5-0604	8μ	4.8	27.6	24.6-30.4
	12μ	5.3	36.4	33.0-39.8
A6-0648	8μ	4.0	25.0	22.4-27.4
	12μ	5.1	35.0	31.6-38.4
A7-0009	8μ	3.5	24.0	21.2-26.8
	12μ	4.1	27.6	25.0-30.4
		Uncoated Boards		
B1-0228	8μ	7.3	43.2	39.8-47.4
	12μ	8.8	44.0	39.4-48.4
B2-1369	8μ	3.3	23.8	21.8-26.0
	12μ	4.1	29.8	26.8-32.6
B3-0185	8μ	5.3	36.4	33.0-39.8
	12μ	7.1	42.6	38.4-46.8
B4-0943	8μ	5.5	34.4	30.6-38.0
	12μ	7.3	48.4	43.6-53.0
B5-0514	8μ	4.4	29.2	26.4-31.8
	12μ	5.5	34.4	30.6-38.0
B6-0878	8μ	2.6	17.6	15.6-19.6
	12μ	1.8	11.4	10.2-12.8

Table IV: Specular Reflectance, ρ_{spec}, and Value and Range of Facet Area, a, for Print Samples at 85° Incidence, In the Machine Direction

Board	Print	ρ_{spec}, %	a, μ^2	a range, μ^2
		Coated Boards		
A1-0485	8μ	9.3	5.30	4.78-5.82
	12μ	13.1	5.92	5.34-6.52
A2-0189	8μ	12.8	5.80	5.20-6.38
	12μ	24.9	13.4	12.0-14.7
A3-0248	8μ	16.7	7.28	6.54-8.02
	12μ	17.8	8.94	8.04-9.84
A4-0750	8μ	21.3	9.64	8.68-10.6
	12μ	22.6	10.2	9.20-11.2
A5-0604	8μ	12.8	6.44	5.78-7.08
	12μ	14.4	7.52	5.88-7.16
A6-0648	8μ	13.6	5.12	4.60-5.64
	12μ	12.8	7.60	6.82-8.38
A7-0009	8μ	12.6	5.70	5.12-6.28
	12μ	9.4	5.36	4.84-5.88
		Uncoated Boards		
B1-0228	8μ	12.3	5.56	5.02-6.12
	12μ	16.9	6.36	5.72-7.00
B2-1369	8μ	6.9	3.70	3.32-4.08
	12μ	9.3	5.30	4.78-5.84
B3-0185	8μ	9.1	4.12	3.70-4.52
	12μ	11.2	4.88	4.42-5.36
B4-0943	8μ	8.9	5.06	4.56-5.64
	12μ	16.5	9.80	8.80-10.8
B5-0514	8μ	8.3	4.92	4.44-5.40
	12μ	12.0	6.44	5.80-7.08
B6-0878	8μ	8.2	4.40	3.96-4.82
	12μ	7.1	3.80	3.42-4.18

Table V: Comparison of Experimental and Calculated Reflectance Maxima, $\rho_{max,e}$ and $\rho_{max,c}$, for Print Samples at 75° Incidence, In the Machine Direction

Board	Print	$\rho_{max,e}$, %	$\rho_{max,e}$ range,%	$\rho_{max,c}$%	$\rho_{max,c}$ range,%
		Coated Boards			
A1-0485	8μ	7.7	6.9-8.5	6.8	6.2-7.5
	12μ	10.3	9.3-11.3	8.5	7.7-9.4
A2-0189	8μ	9.6	8.6-10.6	5.5	5.0-6.1
	12μ	16.8	15.1-18.5	7.4	6.7-8.2
A3-0248	8μ	10.3	9.3-11.3	9.2	8.2-10.2
	12μ	14.6	13.1-16.1	11.0	10.3-12.2
A4-0750	8μ	14.4	13.0-15.8	10.6	9.5-11.7
	12μ	16.7	15.0-18.4	5.4	4.9-6.0
A5-0604	8μ	7.2	6.5-7.9	5.2	4.7-6.0
	12μ	10.6	9.5-11.7	6.0	5.4-6.5
A6-0648	8μ	8.0	7.2-8.8	4.4	4.0-4.9
	12μ	9.0	8.1-9.9	5.7	5.2-6.3
A7-0009	8μ	6.6	5.9-7.3	3.9	3.5-4.4
	12μ	6.6	5.9-7.3	4.6	4.2-5.1
		Uncoated Boards			
B1-0228	8μ	9.5	8.5-10.5	7.9	7.3-8.7
	12μ	11.5	10.3-12.7	9.4	8.4-10.3
B2-1369	8μ	4.6	4.1-5.1	3.7	3.4-4.1
	12μ	6.0	5.4-6.6	4.7	4.2-5.1
B3-0185	8μ	7.0	6.3-7.7	6.0	5.4-6.5
	12μ	9.6	8.6-10.6	7.6	6.8-8.3
B4-0943	8μ	7.2	6.5-7.9	6.1	5.4-6.7
	12μ	12.2	11.0-13.4	8.1	7.3-8.9
B5-0514	8μ	6.0	5.4-6.6	4.9	4.4-5.3
	12μ	8.0	7.2-8.8	6.1	5.4-6.7
B6-0878	8μ	3.6	3.2-4.0	2.9	2.6-3.3
	12μ	2.6	2.3-2.9	2.0	1.8-2.2

Table VI: Comparison of Experimental and Calculated Reflectance Maxima, $\rho_{max,e}$ and $\rho_{max,c}$, for Print Samples at 85° Incidence, In the Machine Direction

Board	Print	$\rho_{max,e}$,%	$\rho_{max,e}$ range,%	$\rho_{max,c}$,%	$\rho_{max,c}$ range,%
		Coated Boards			
A1-0485	8μ	13.0	11.7-14.3	9.8	8.9-10.8
	12μ	15.4	13.9-16.9	13.6	12.3-15.0
A2-0189	8μ	16.2	14.6-17.8	13.3	12.0-14.7
	12μ	32.3	29.1-35.5	26.2	23.6-28.8
A3-0248	8μ	19.1	17.2-21.0	17.3	15.5-19.1
	12μ	23.3	21.0-25.6	18.6	16.7-20.4
A4-0750	8μ	25.6	23.0-28.2	22.2	19.9-24.4
	12μ	29.4	26.5-32.3	23.6	21.2-26.0
A5-0604	8μ	20.5	18.4-22.6	13.4	12.0-14.7
	12μ	15.0	13.5-16.5	15.0	13.5-16.5
A6-0648	8μ	15.9	14.3-17.5	13.9	12.5-15.3
	12μ	17.6	15.8-19.4	13.6	12.2-15.0
A7-0009	8μ	16.5	14.8-18.2	13.1	11.8-14.4
	12μ	16.1	14.5-17.7	10.0	9.0-11.0
		Uncoated Boards			
B1-0228	8μ	14.6	13.1-16.1	12.8	11.5-14.1
	12μ	18.0	16.2-19.8	17.3	15.5-19.0
B2-1369	8μ	7.6	6.8-8.4	7.3	6.5-8.0
	12μ	11.7	10.5-12.9	9.9	8.9-10.9
B3-0185	8μ	10.2	9.2-11.2	9.5	8.5-10.4
	12μ	11.6	10.4-12.8	11.6	10.4-12.8
B4-0943	8μ	10.5	9.4-11.6	9.4	8.5-10.5
	12μ	21.8	19.6-24.0	17.5	15.7-19.3
B5-0514	8μ	14.6	13.1-16.1	8.8	7.9-9.6
	12μ	15.7	14.1-17.3	12.6	11.4-13.9
B6-0878	8μ	12.2	11.0-13.4	8.6	7.8-9.5
	12μ	11.5	10.3-12.7	7.5	6.7-8.2

Table VII: Position of Reflectance Maximum, θ_{max}, and Value and Range of Standard Deviation, σ, for Print Samples at 75° Incidence, Across the Machine Direction

Board	Print	θ_{max}, deg.	σ, deg.	σ range, deg.
		Coated Boards		
A1-0485	8μ	80.0	5.30	4.75-5.80
	12μ	80.5	5.50	5.00-6.00
A2-0189	8μ	79.25	4.80	4.25-5.40
	12μ	80.0	5.30	4.75-5.80
A3-0248	8μ	80.0	5.30	4.75-5.80
	12μ	79.25	4.80	4.25-5.40
A4-0750	8μ	79.75	5.10	4.60-5.70
	12μ	79.5	5.00	4.40-5.50
A5-0604	8μ	79.0	4.75	4.10-5.30
	12μ	78.25	4.30	3.60-4.80
A6-0648	8μ	79.0	4.75	4.10-5.30
	12μ	79.0	4.75	4.10-5.30
A7-0009	8μ	79.25	4.80	4.25-5.40
	12μ	79.0	4.75	4.10-5.30
		Uncoated Boards		
B1-0228	8μ	79.25	4.80	4.25-5.40
	12μ	79.75	5.10	4.60-5.70
B2-1369	8μ	80.0	5.30	4.75-5.80
	12μ	80.5	5.50	5.00-6.00
B3-0185	8μ	80.5	5.50	5.00-6.00
	12μ	79.5	5.00	4.40-5.50
B4-0943	8μ	79.75	5.10	4.60-5.70
	12μ	79.0	4.75	4.10-5.30
B5-0514	8μ	81.0	5.80	5.30-6.20
	12μ	80.0	5.30	4.75-5.80
B6-0878	8μ	80.0	5.30	4.75-5.80
	12μ	80.0	5.30	4.75-5.80

Table VIII: Position of Reflectance Maximum, θ_{max}, and Value and Range of Standard Deviation, σ, for Print Samples at 85° Incidence, Across the Machine Direction

Board	Print	θ_{max}, deg.	σ, deg.	σ range, deg.
		Coated Boards		
A1-0485	8μ	87.5	3.55	2.70-
	12μ	86.5	2.70	1.60-3.55
A2-0189	8μ	87.75	3.70	3.00-
	12μ	88.0	4.00	3.20-
A3-0248	8μ	88.0	4.00	3.20-
	12μ	88.0	4.00	3.20-
A4-0750	8μ	88.25	4.20	3.40-
	12μ	88.0	4.00	3.20-
A5-0604	8μ	87.75	3.70	3.00-
	12μ	87.0	3.20	2.25-
A6-0648	8μ	87.5	3.55	2.70-
	12μ	87.5	3.55	2.70-
A7-0009	8μ	87.75	3.70	3.00-
	12μ	88.0	4.00	3.20-
		Uncoated Boards		
B1-0228	8μ	88.75		
	12μ	88.25	4.20	3.40-
B2-1369	8μ	87.5	3.55	2.70-
	12μ	88.25	4.20	3.40-
B3-0185	8μ	88.25	4.20	3.40-
	12μ	88.5		
B4-0943	8μ	88.75		
	12μ	88.0	4.00	3.20-
B5-0514	8μ	89.0		
	12μ	89.0		
B6-0878	8μ	88.25	4.20	3.40-
	12μ	89.0		

Table IX: Specular Reflectance, ρ_{spec}, and Value and Range of Facet Area, a, for Print Samples at 75° Incidence, Across the Machine Direction

Board	Print	ρ_{spec}, %	a, μ^2	a range, μ^2
		Coated Boards		
A1-0485	8μ	4.9	32.4	29.2-35.8
	12μ	5.2	35.8	32.4-39.2
A2-0189	8μ	5.6	33.6	30.0-37.2
	12μ	5.9	39.0	35.2-41.2
A3-0248	8μ	6.4	42.4	38.4-46.4
	12μ	7.2	43.2	39.0-47.4
A4-0750	8μ	7.4	47.2	42.8-51.6
	12μ	8.1	50.6	45.0-55.6
A5-0604	8μ	5.6	33.2	29.6-36.8
	12μ	6.6	35.4	31.8-39.2
A6-0648	8μ	5.7	33.8	30.2-37.4
	12μ	5.2	30.8	28.0-33.8
A7-0009	8μ	5.2	31.2	28.2-34.2
	12μ	5.1	30.2	27.2-33.2
		Uncoated Boards		
B1-0228	8μ	5.4	32.4	29.4-35.4
	12μ	6.0	38.2	34.4-42.0
B2-1369	8μ	3.1	21.0	18.6-23.2
	12μ	3.1	21.2	19.2-23.4
B3-0185	8μ	3.7	25.4	22.8-28.2
	12μ	5.5	34.4	30.6-38.2
B4-0943	8μ	4.2	26.8	24.2-29.2
	12μ	6.1	36.2	32.6-39.8
B5-0514	8μ	3.0	21.8	19.6-24.0
	12μ	4.7	31.2	27.8-34.4
B6-0878	8μ	3.0	19.8	17.8-21.8
	12μ	2.8	18.6	16.6-21.2

Table X: Specular Reflectance, ρ_{spec}, and Value and Range of Facet Area, a, for Print Samples at 85° Incidence, Across the Machine Direction

Board	Print	ρ_{spec}, %	a, μ^2	a range, μ^2
		Coated Boards		
A1-0485	8μ	8.1	4.82	4.36-5.30
	12μ	9.9	4.48	4.02-4.92
A2-0189	8μ	9.9	6.12	5.52-6.76
	12μ	10.0	6.68	6.02-7.36
A3-0248	8μ	10.0	6.68	6.02-7.36
	12μ	11.7	7.84	7.02-8.62
A4-0750	8μ	9.2	6.48	5.84-7.12
	12μ	12.2	8.18	7.36-8.98
A5-0604	8μ	7.8	4.84	4.34-5.32
	12μ	10.0	5.36	4.84-5.90
A6-0648	8μ	9.3	5.52	5.00-6.04
	12μ	9.9	5.88	5.28-6.46
A7-0009	8μ	9.4	5.82	5.26-6.38
	12μ	8.2	5.48	4.96-6.02
		Uncoated Boards		
B1-0228	8μ	7.5		
	12μ	8.8	6.20	5.56-6.82
B2-1369	8μ	6.2	3.68	3.32-4.04
	12μ	5.7	4.02	3.62-4.44
B3-0185	8μ	7.0	4.92	4.44-5.44
	12μ	8.9		
B4-0943	8μ	6.0		
	12μ	8.2	5.48	4.96-6.02
B5-0514	8μ	4.5		
	12μ	5.1		
B6-0878	8μ	5.5	3.88	3.46-4.30
	12μ	4.8		

Table XI: Comparison of Experimental and Calculated Reflectance Maxima, $\rho_{max,e}$ and $\rho_{max,c}$, for Print Samples at 75° Incidence, Across the Machine Direction

Board	Print	$\rho_{max,e}$,%	$\rho_{max,e}$ range,%	$\rho_{max,c}$,%	$\rho_{max,c}$ range,%
		Coated Boards			
A1-0485	8μ	6.8	6.1-7.5	5.5	4.9-6.1
	12μ	7.9	7.1-8.7	5.9	5.3-6.5
A2-0189	8μ	8.4	7.6-9.2	6.1	5.5-6.8
	12μ	11.2	10.1-12.3	6.5	5.9-6.9
A3-0248	8μ	10.0	9.0-11.0	7.1	6.5-7.8
	12μ	13.3	12.0-14.6	7.9	7.1-8.7
A4-0750	8μ	14.6	13.1-16.1	8.2	7.5-9.0
	12μ	17.8	16.0-19.6	9.0	8.0-9.9
A5-0604	8μ	8.7	7.8-9.6	6.1	5.4-6.8
	12μ	9.0	8.1-9.9	7.1	6.4-7.9
A6-0648	8μ	9.3	8.4-10.2	6.2	5.5-6.9
	12μ	8.5	7.6-9.4	5.7	5.1-6.2
A7-0009	8μ	7.0	6.3-7.7	5.7	5.2-6.3
	12μ	6.8	6.1-7.5	5.5	5.0-6.1
		Uncoated Boards			
B1-0228	8μ	6.8	6.1-7.5	5.9	5.4-6.5
	12μ	9.2	8.3-10.1	6.7	6.0-7.3
B2-1369	8μ	3.8	3.4-4.2	3.5	3.1-3.9
	12μ	3.9	3.5-4.3	3.5	3.1-3.9
B3-0185	8μ	4.9	4.4-5.4	4.2	3.8-4.6
	12μ	7.3	6.6-8.0	6.1	5.5-6.7
B4-0943	8μ	5.0	4.5-5.5	4.7	4.2-5.2
	12μ	8.1	7.3-8.9	6.6	5.9-7.3
B5-0514	8μ	4.3	3.9-4.7	3.4	3.1-3.7
	12μ	7.2	6.5-7.9	5.2	4.7-5.7
B6-0878	8μ	4.2	3.8-4.6	3.3	3.0-3.6
	12μ	3.8	3.4-4.2	3.1	2.8-3.4

Table XII: Comparison of Experimental and Calculated Reflectance Maxima, $\rho_{max,e}$ and $\rho_{max,c}$, for Print Samples at 85° Incidence, Across the Machine Direction

Board	Print	$\rho_{max,e}$,%	$\rho_{max,e}$ range,%	$\rho_{max,c}$,%	$\rho_{max,c}$ range,%
		Coated Boards			
A1-0485	8μ	13.6	12.2-15.0	8.6	7.7-9.5
	12μ	11.4	10.3-12.5	10.3	9.3-11.3
A2-0189	8μ	18.2	16.4-20.0	10.6	9.5-11.7
	12μ	23.2	21.0-25.6	11.1	10.0-12.2
A3-0248	8μ	18.4	16.6-20.2	11.1	10.0-12.2
	12μ	23.0	20.7-25.3	12.7	11.4-14.0
A4-0750	8μ	19.8	17.8-21.8	10.1	9.1-11.1
	12μ	24.3	21.9-26.7	13.2	11.9-14.5
A5-0604	8μ	18.2	16.4-20.0	8.4	7.6-9.2
	12μ	16.7	15.0-18.4	10.5	9.4-11.6
A6-0648	8μ	17.4	15.7-19.1	9.9	8.9-10.9
	12μ	17.4	15.7-19.1	10.5	9.4-11.6
A7-0009	8μ	15.8	14.2-17.4	10.1	9.1-11.1
	12μ	16.7	15.0-18.4	8.9	8.0-9.8
		Uncoated Boards			
B1-0228	8μ	14.9	13.4-16.4		
	12μ	16.6	14.9-18.3	9.6	8.6-10.6
B2-1369	8μ	8.4	7.6-9.2	6.6	5.9-7.3
	12μ	7.9	7.1-8.7	6.2	5.6-6.8
B3-0185	8μ	12.7	11.4-14.0	7.6	6.8-8.4
	12μ	13.4	12.7-14.7		
B4-0943	8μ	10.8	9.7-11.9		
	12μ	14.8	13.3-16.3	8.9	8.0-9.8
B5-0514	8μ	12.9	11.6-14.2		
	12μ	15.8	14.2-17.4		
B6-0878	8μ	13.7	12.3-15.1	6.0	5.4-6.6
	12μ	13.2	11.9-14.5		

REFERENCES

1. Fetsko, J. M., and Zettlemoyer, A. C., TAPPI 45, 667 (1962)
2. Zettlemoyer, A.C., Penrose Annual 56, 116 (1962)
3. Schaeffer, W. D., Amer. Ink Maker 45, 70 (1967)
4. Hunter, R. S., J. Res. Nat. Bur. Stds. 18, 19 (1937)
5. Bouguer, P., Histoire de l' Académie Royale des Sciences, Paris, 1757
6. Grabowski, L., Astrophys. J. 39, 299 (1914)
7. Jenkins, F. A., and White, H. E., "Fundamentals of Optics," McGraw Hill Book Company, New York. 1950. 2nd edition. pp.560-564
8. Berry, E. M., J. Opt. Soc. Amer. 7, 627 (1923)
9. Chinmayanandam, L. K., Phys. Rev., Sec. II, 13, 96 (1919)
10. Pokrowski, G. I., Z. Phys. 30, 66 (1924)
11. Pokrowski, G. I., Z. Phys. 35, 34 (1925)
12. Pokrowski, G. I., Z. Phys. 35, 390 (1926)
13. Pokrowski, G. I., Z. Phys. 36, 472 (1926)
14. Schulz, H., Z. Phys. 31, 496 (1925)
15. Barkas, W. W., Proc. Phys. Soc. 51, 274 (1939)
16. Bennett, H. E., and Porteus, J. O., J. Opt. Soc. Amer. 51, 123 (1961)
17. Bennett, H. E., J. Opt. Soc. Amer. 53, 1389 (1963)
18. Porteus, J. O., J. Opt. Soc. Amer. 53, 1394 (1963)
19. Gordinskii, G. M., Optics and Spectrosc. 15, 57 (1963)
20. Toporets, A. S., Optics and Spectrosc. 16, 54 (1964)
21. Polyanskii, V. K., and Rvachev, V. P., Optics and Spectrosc. 20, 391 (1966)
22. Voishvillo, N. A., Optics and Spectrosc. 22, 517 (1967)
23. Toporets, A. S., Optics and Spectrosc. 24, 62 (1968)
24. Polyanskii, V. K., Kovalskii, L. V., and Milovidova, T. I., Optics and Spectrosc. 25, 415 (1968)
25. Nelson, H. F., and Goulard, R., J. Opt. Soc. Amer. 57, 769 (1967)
26. Birkebak, R. C., Sparrow, E. M., Eckert, E. R. G., and Ramsey, J. W., J. Heat Trans. 86, Ser. C, 193 (1964)

27. Birkebak, R. C., and Eckert, E. R. G., J. Heat Trans. 87, Ser. C, 85 (1965)

28. Torrance, K. E., and Sparrow, E. M., J. Heat Trans. 87, Ser. C, 93 (1965)

29. Torrance, K. E., and Sparrow, E. M., J. Heat Trans. 87, Ser. C, 283 (1965)

30. Torrance, K. E., and Sparrow, E. M., J. Heat Trans. 88, Ser. C, 223 (1966)

31. Torrance, K. E., Sparrow, E. M., and Birkebak, R. C., J. Opt. Soc. Amer. 56, 916 (1966)

32. Birkebak, R. C., Dawson, J. P., McCullough, B. A., and Wood, B. E., Int. J. Heat Mass Trans. 10, 1225 (1967)

33. Torrance, K. E., and Sparrow, E. M., J. Opt. Soc. Amer. 57, 1105 (1967)

34. Wood, R. W., "Physical Optics", Dover Publications, New York. 1967. 3rd revised edition. pp. 39-41

35. Harrison, V. G. W., "Definition and Measurement of Gloss", Patra, Surrey, England. 1945

36. Born, M., and Wolf, E., "Principles of Optics", Pergamon Press, Oxford. 1964. 2nd revised edition. pp. 181-185

37. Judd, D. B., J. Opt. Soc. Amer. 57, 445 (1967)

38. Rense, W. A., J. Opt. Soc. Amer. 40, 55 (1950)

39. Freund, J. E., "Mathematical Statistics", Prentice-Hall, Inc., Englewood Cliffs, N. J.. 1962 pp. 147-148

40. Parzen, E., "Modern Probability Theory and Its Applications", John Wiley & Sons, Inc., New York. 1960. p. 188

41. Torrance, K. E., J. Heat Trans. 91, Ser. C, 287 (1969)

42. Harrison, V. G. W., Brit. J. Appl. Phys. 1, 46 (1950)

43. Persson, L., private communication

VITA

Frederick Everett Witherell, Jr., was born in Elizabeth, New Jersey on August 15, 1946. He attended public grammar schools in Chicago, Illinois and Elizabeth, New Jersey, and high school in Elizabeth, New Jersey. He attended Lehigh University, and received the degree of Bachelor of Science in Chemical Engineering in 1968. He began graduate study at Lehigh later that same year, with a research assistantship in Chemical Engineering.